Electronic Supplementary Material (ESI) for Polymer Chemistry.

SUPPORTING INFORMATION

Allyl amino-Thioxanthone Derivatives as Highly Efficient Visible Light H-Donor and Co-polymerizable Photoinitiators

Louise Breloy[†], Raúl Losantos[§], Diego Sampedro[§], Marco Marazzi[Φ, Δ], Jean-Pierre Malval[≠], Yun Heo, Jun Akimoto, Yoshihiro Ito[‡], Vlasta Brezová[±], Davy-Louis Versace[†]*

FIGURES

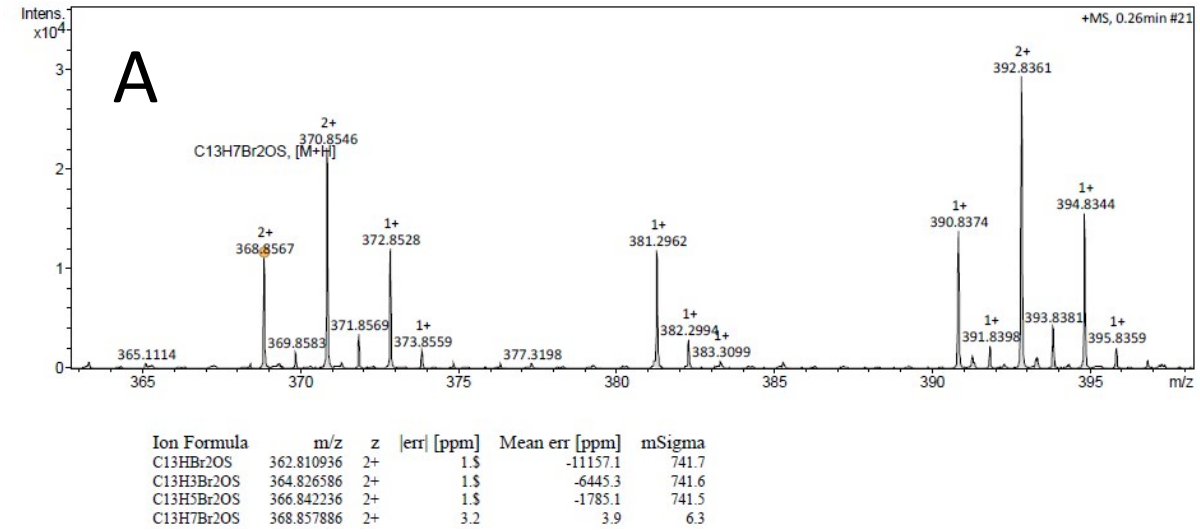

Ion Formula	m/z	z	|err| [ppm]	Mean err [ppm]	mSigma
C13HBr2OS	362.810936	2+	1.$	-11157.1	741.7
C13H3Br2OS	364.826586	2+	1.$	-6445.3	741.6
C13H5Br2OS	366.842236	2+	1.$	-1785.1	741.5
C13H7Br2OS	368.857886	2+	3.2	3.9	6.3

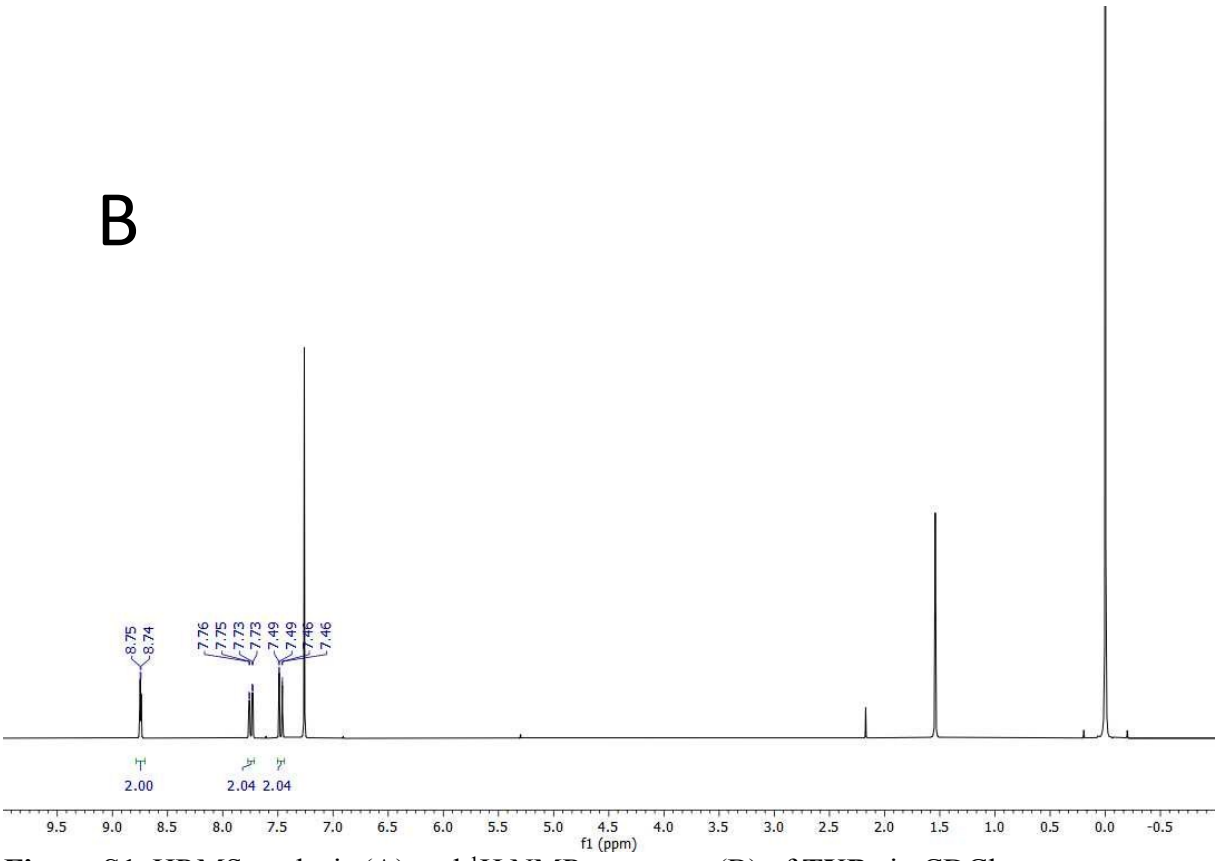

Figure S1. HRMS analysis (A) and ^{1}H NMR spectrum (B) of **TXBr** in $CDCl_3$

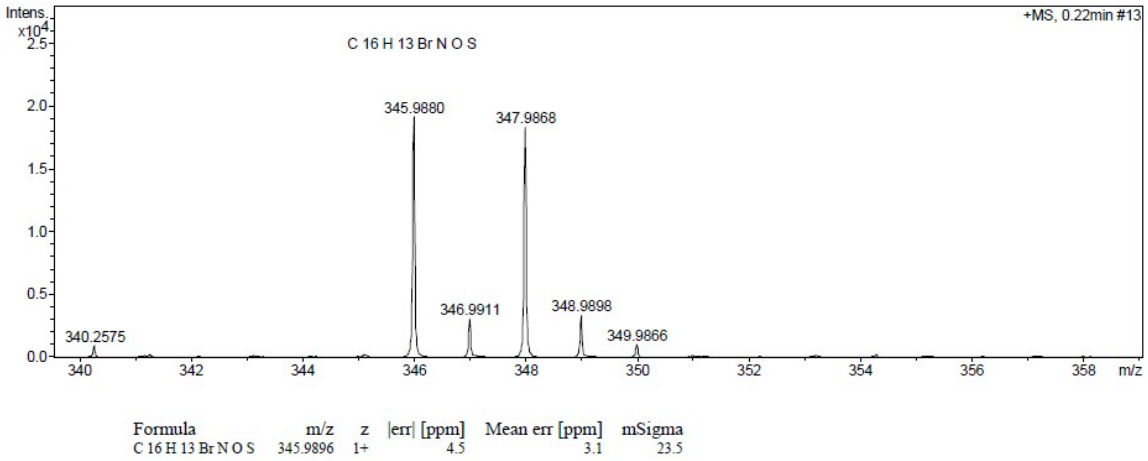

Formula	m/z	z	|err| [ppm]	Mean err [ppm]	mSigma
C 16 H 13 Br N O S	345.9896	1+	4.5	3.1	23.5

Figure S2. HRMS analysis of **TXA**

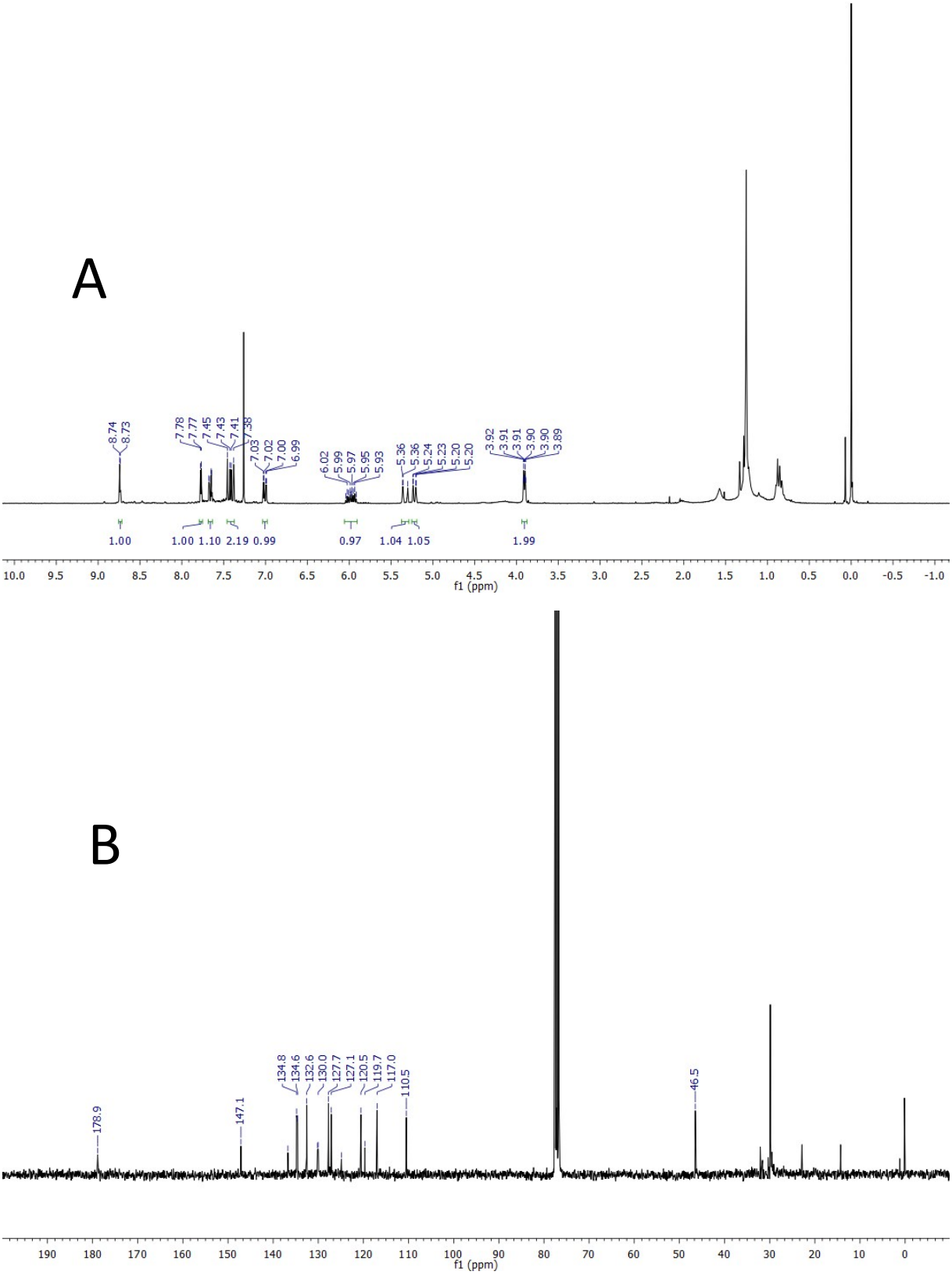

Figure S3. ^{1}H NMR (A) and ^{13}C NMR (B) spectrum of **TXA** in $CDCl_3$

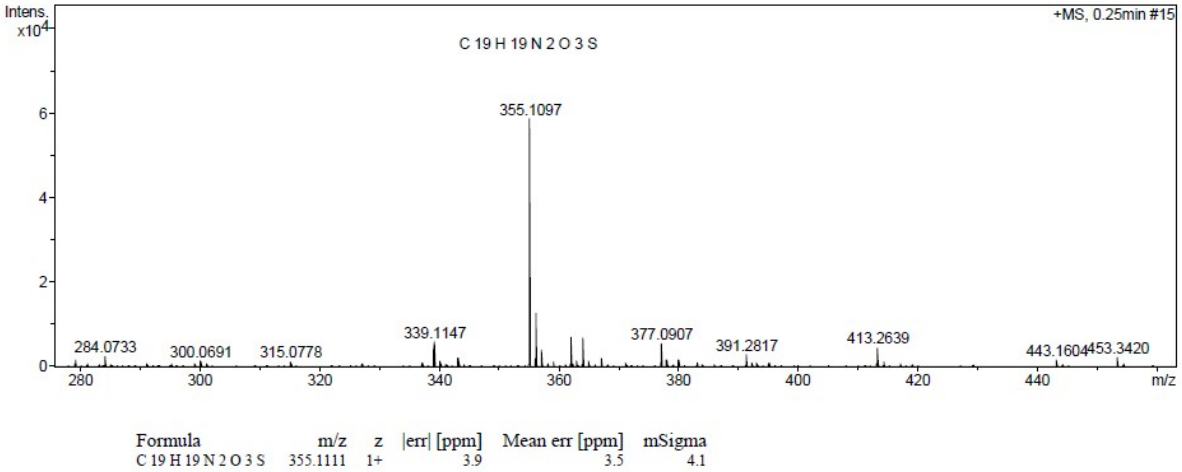

Figure S4. HRMS analysis of **TXo2A**

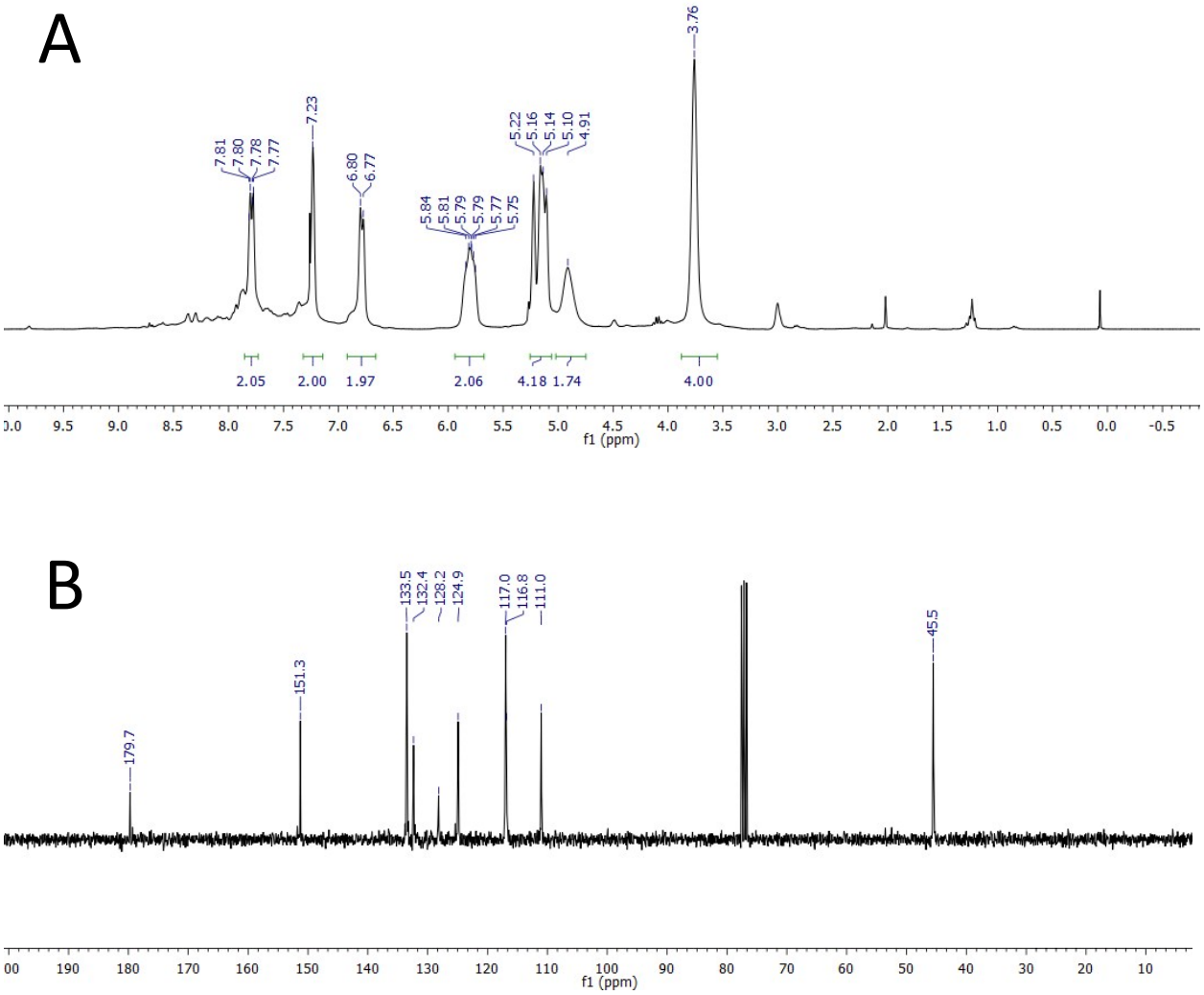

Figure S5. ^{1}H NMR (A) and ^{13}C NMR (B) spectrum of **TXo2A** in $CDCl_3$

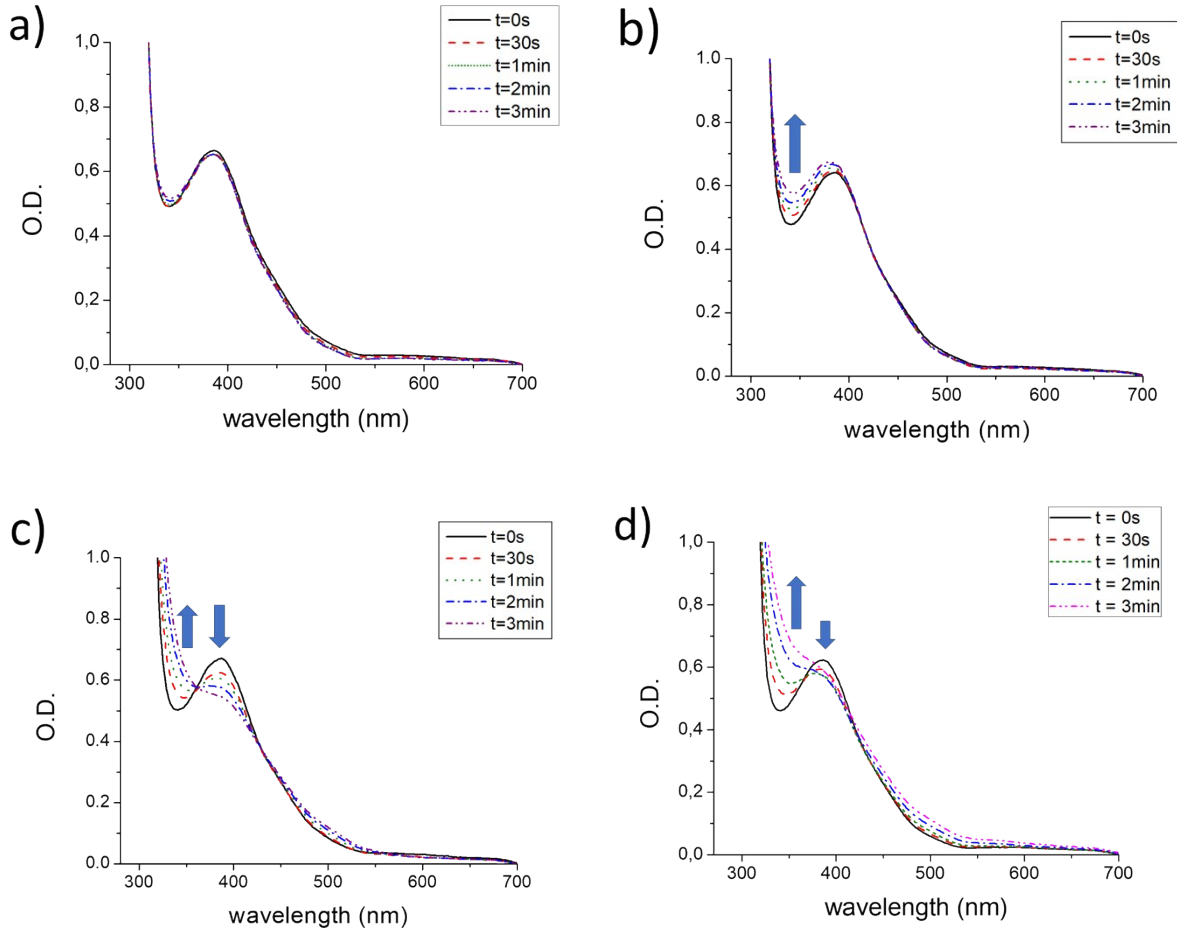

Figure S6. Photolysis under air after light irradiation with a LED 405 nm in ACN in the presence of a) **TXo2A** alone, b) **TXo2A**/Iod system, c) **TXo2A**/MDEA system and d) **TXo2A**/TT system. [**TXo2A**] = 6.7 x 10^{-2} g/L, [Iod] = 3.5 x 10^{-2} g/L, [MDEA] = [TT] = 7 g/L.

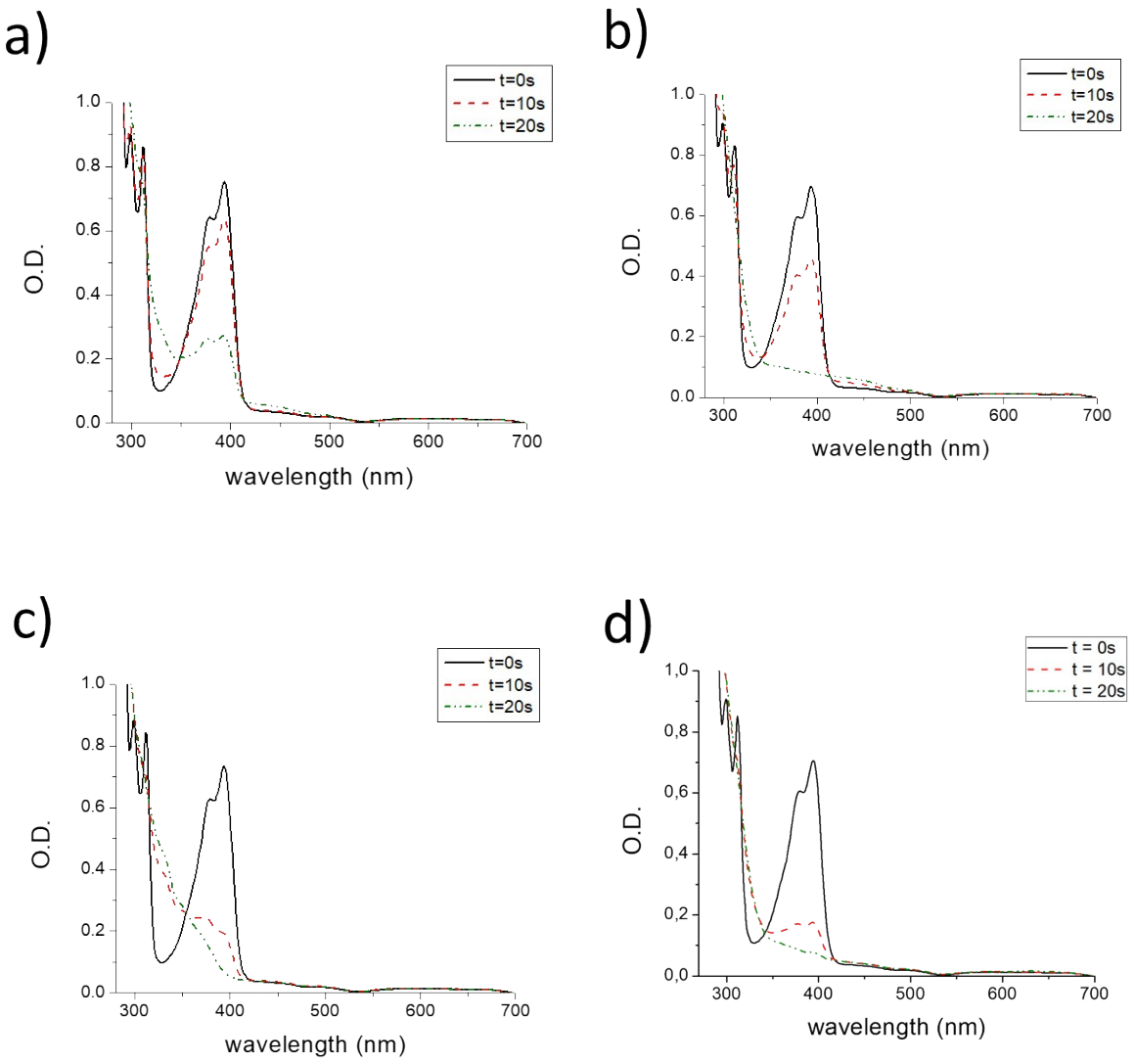

Figure S7. Steady state photolysis under air after LED@405nm exposure in the presence of a) **TXBr** alone, b) **TXBr**/Iod, c) **TXBr**/MDEA, d) **TXBr** /TT. Solvent = THF. [**TXBr**] = 6.7 x 10^{-2} g/L, [Iod] = 3.5 x 10^{-2} g/L, [MDEA] = 2.2 x 10^{-1} g/L and [TT] = 9 x 10^{-2} g/L.

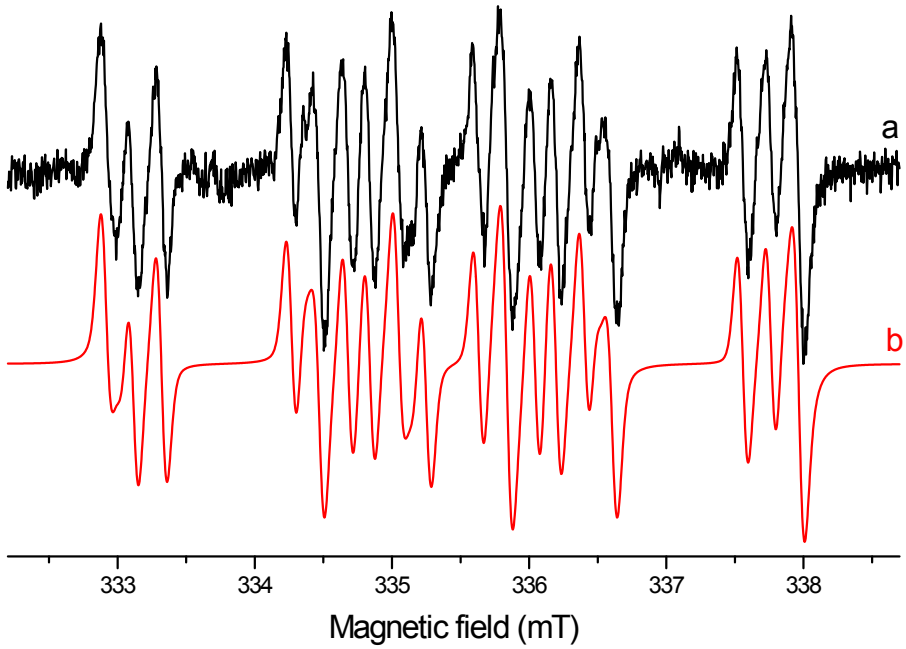

Figure S8. The experimental EPR spectrum (a) along with simulation (b) obtained upon *in situ* LED@400 nm irradiation of argon saturated (**TXA**/DMPO) system in benzene. The multi-component simulation spectrum was calculated considering presence of three DMPO-adducts: •DMPO-CR_1 (a_N = 1.429 mT, a_H = 2.136 mT; g = 2.0059), •DMPO-NR_2 (a_N = 1.370 mT, a_H = 1.941 mT, a_N = 0.206 mT; g = 2.0060) and •DMPO-C(N-alkyl) (a_N = 1.448 mT, a_H = 1.707 mT; g = 2.0060).

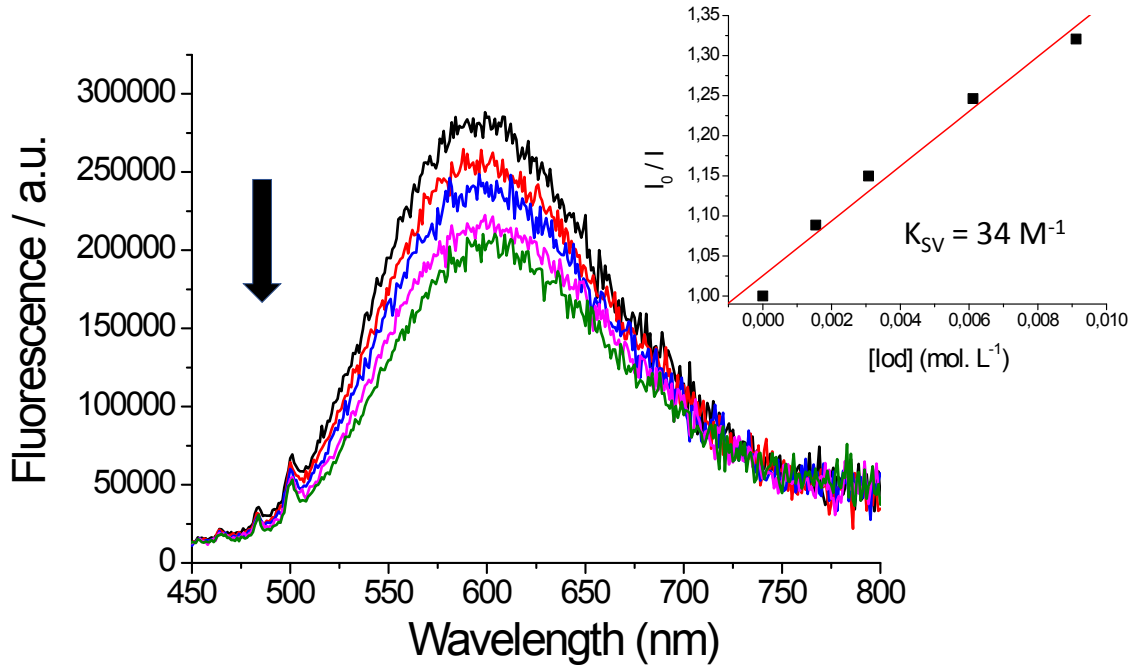

Figure S9. Quenching of the fluorescence of **TXo2A** upon gradual addition of Iod (solvent: ACN). *Inset*: Corresponding Stern-Volmer plot.

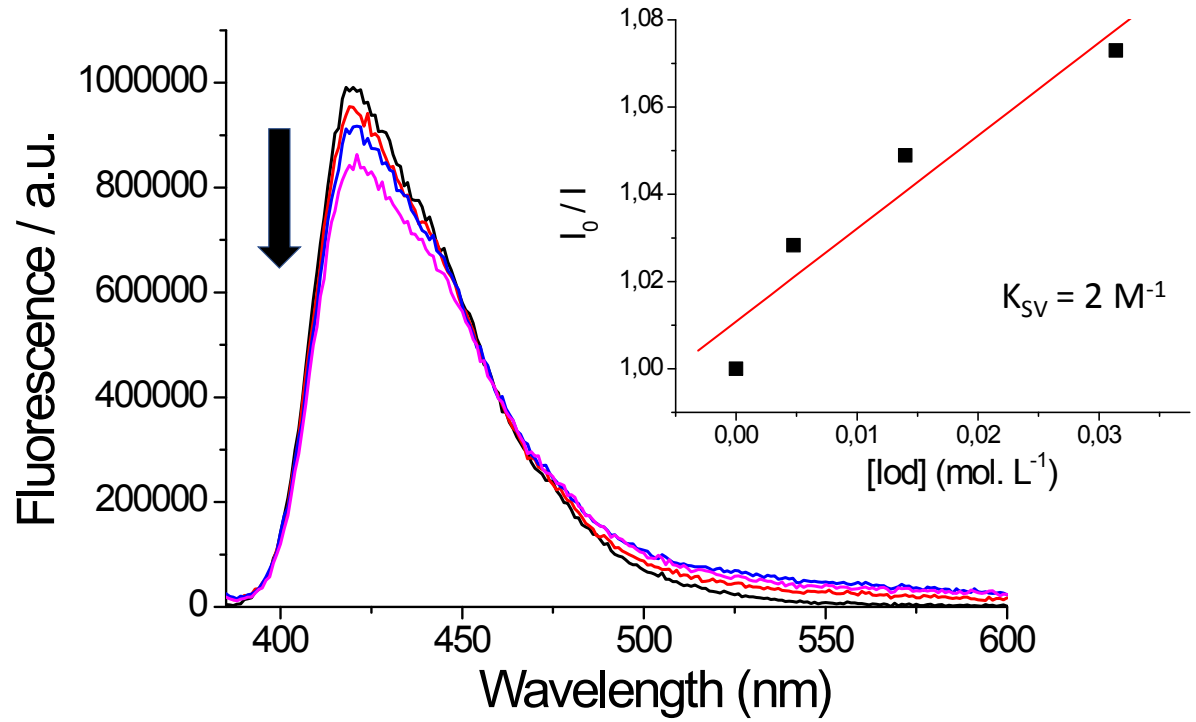

Figure S10. Quenching of the fluorescence of **TXBr** upon gradual addition of Iod (solvent: ACN). *Inset*: Corresponding Stern-Volmer plot.

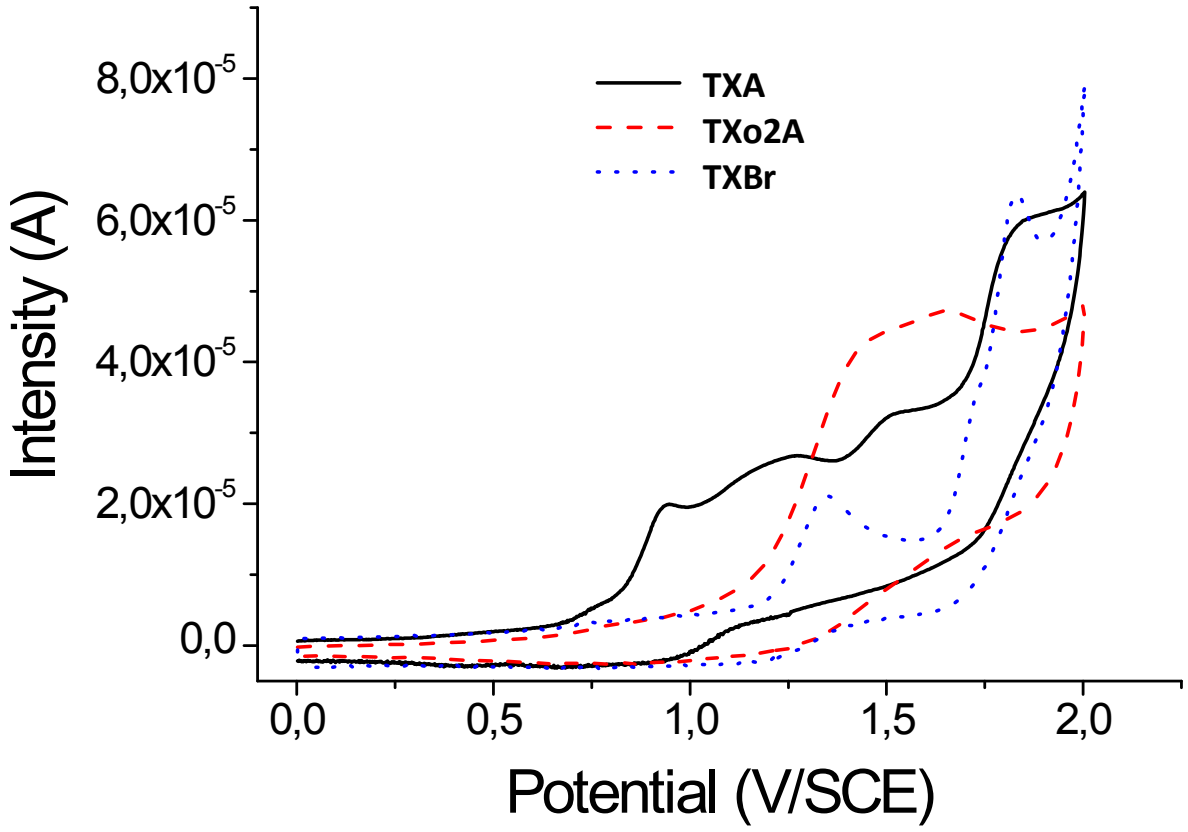

Figure S11. Cyclic voltammograms of **TXA** and **TXo2A** in ACN, and **TXBr** in a mixed solvent THF/ACN (25/75 v/v) + 5 x 10^{-2} M nBu$_4$NPF$_6$ measured at a scan rate of 100 mV.s^{-1}. [**TXA**] = [**TXo2A**] = [**TXBr**] = 10^{-3} M.

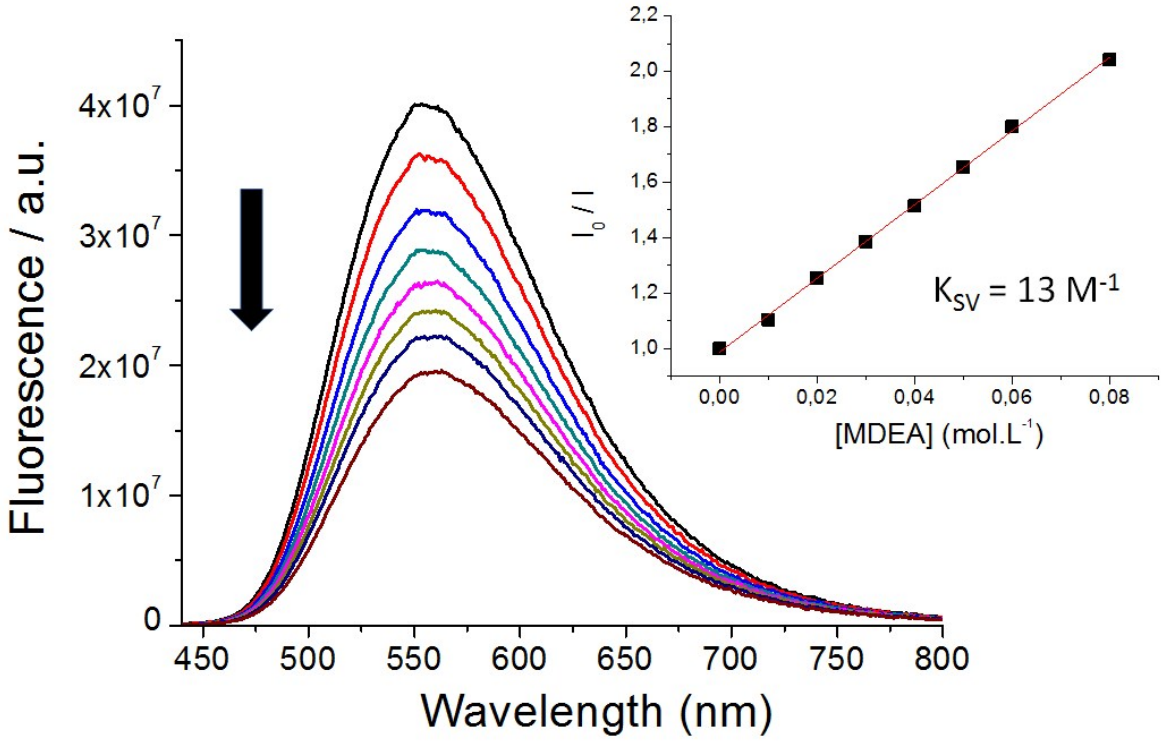

Figure S12. Quenching of the fluorescence of **TXA** upon gradual addition of MDEA (solvent: ACN). *Inset*: Corresponding Stern-Volmer plot.

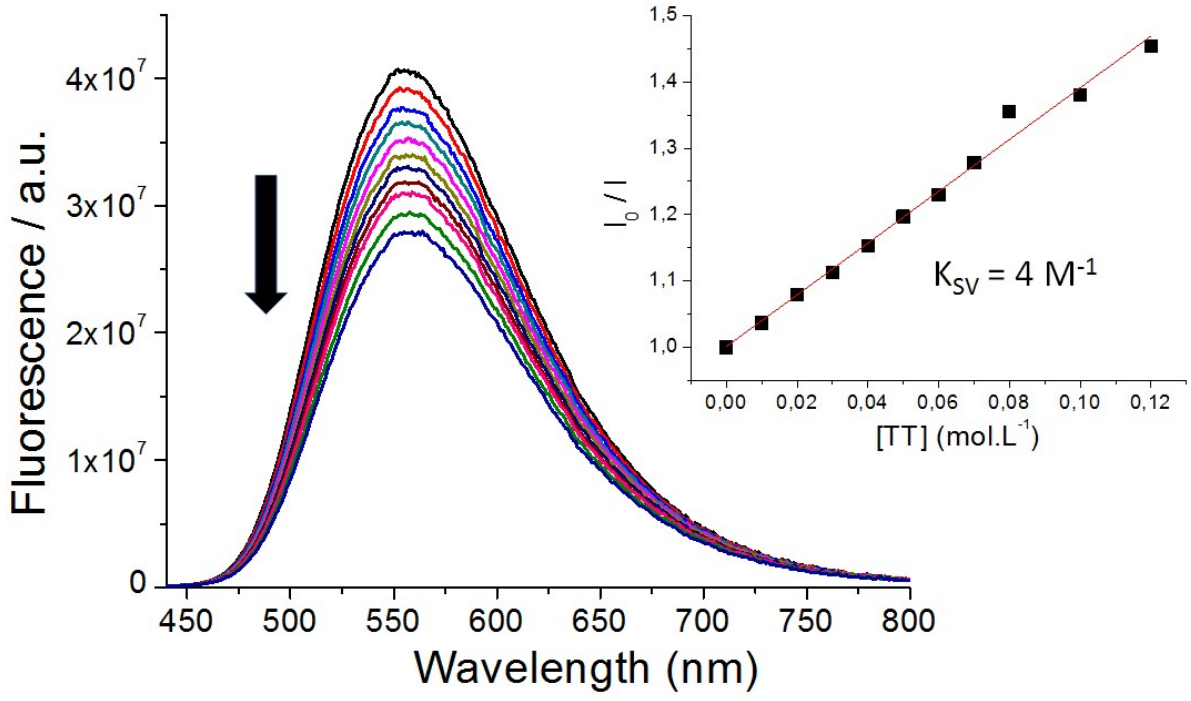

Figure S13. Quenching of the fluorescence of **TXA** upon gradual addition of TT (solvent: ACN). *Inset*: Corresponding Stern-Volmer plot.

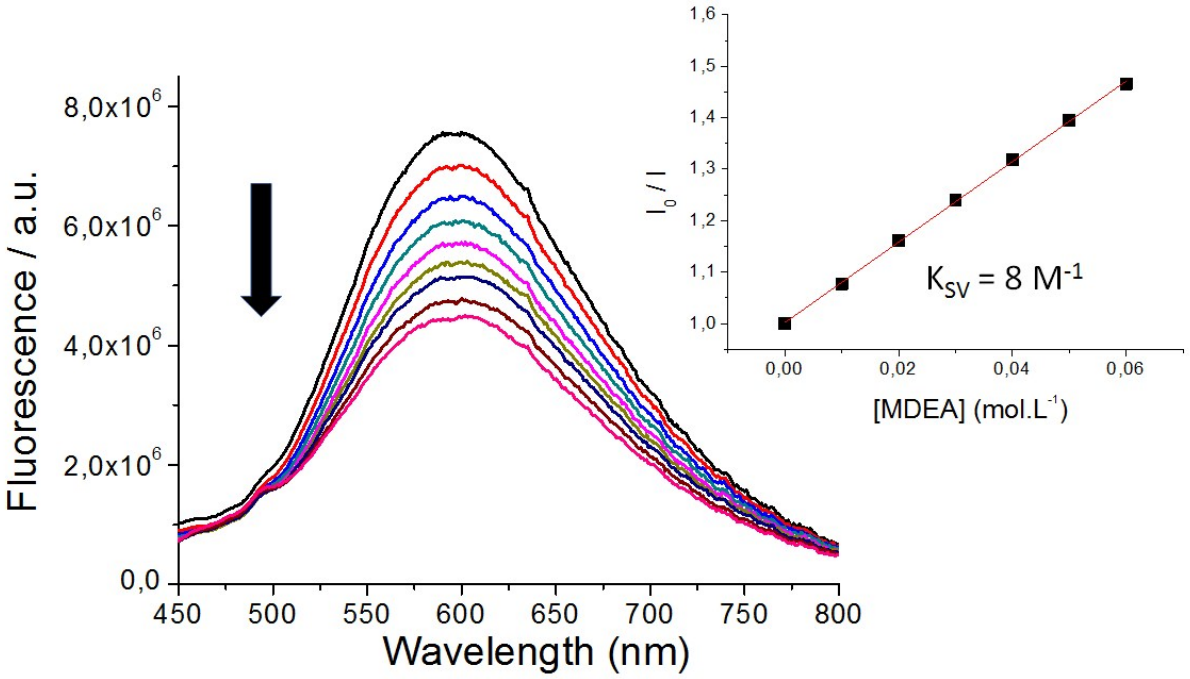

Figure S14. Quenching of the fluorescence of **TXo2A** upon gradual addition of MDEA (solvent: ACN). *Inset*: Corresponding Stern-Volmer plot.

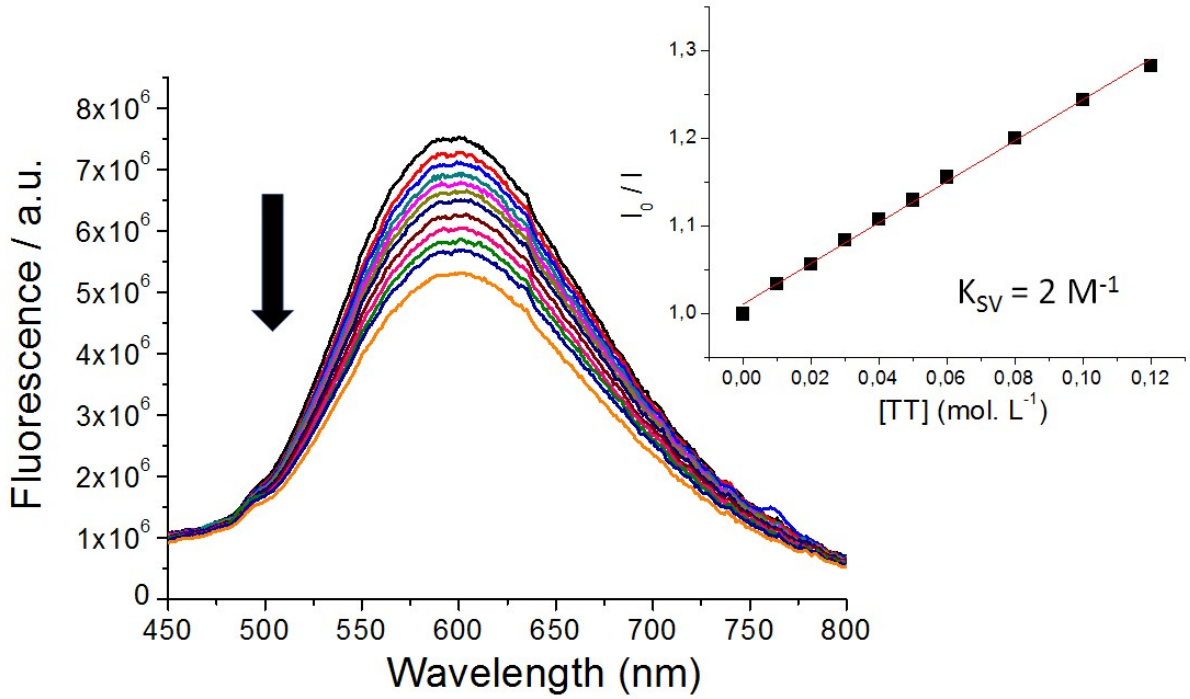

Figure S15. Quenching of the fluorescence of **TXo2A** upon gradual addition of TT (solvent: ACN). *Inset*: Corresponding Stern-Volmer plot.

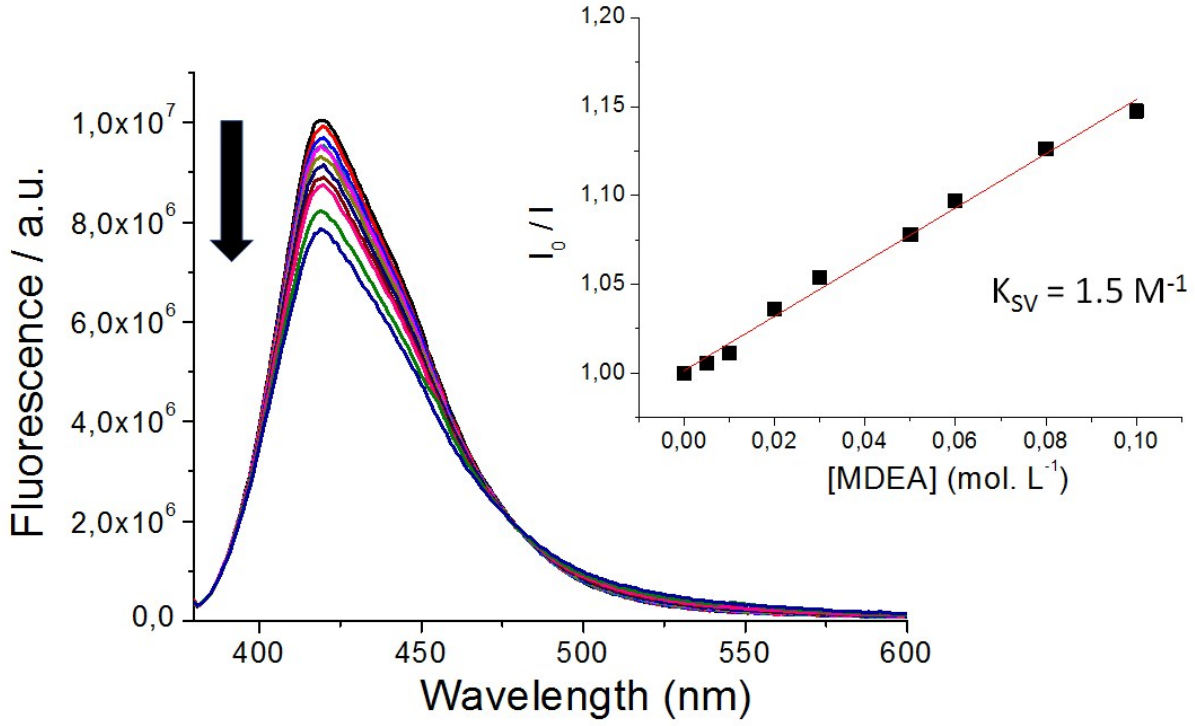

Figure S16. Quenching of the fluorescence of **TXBr** upon gradual addition of MDEA (solvent: ACN). *Inset*: Corresponding Stern-Volmer plot.

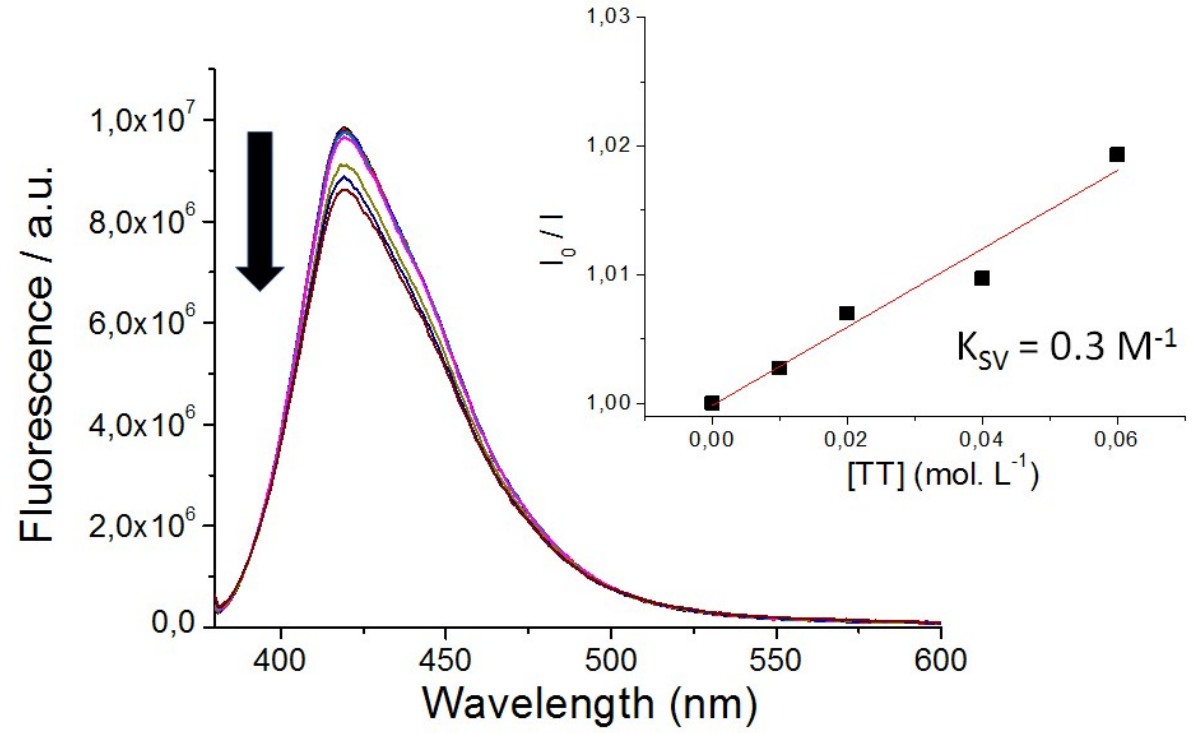

Figure S17. Quenching of the fluorescence of **TXBr** upon gradual addition of TT (solvent: ACN). *Inset*: Corresponding Stern-Volmer plot.

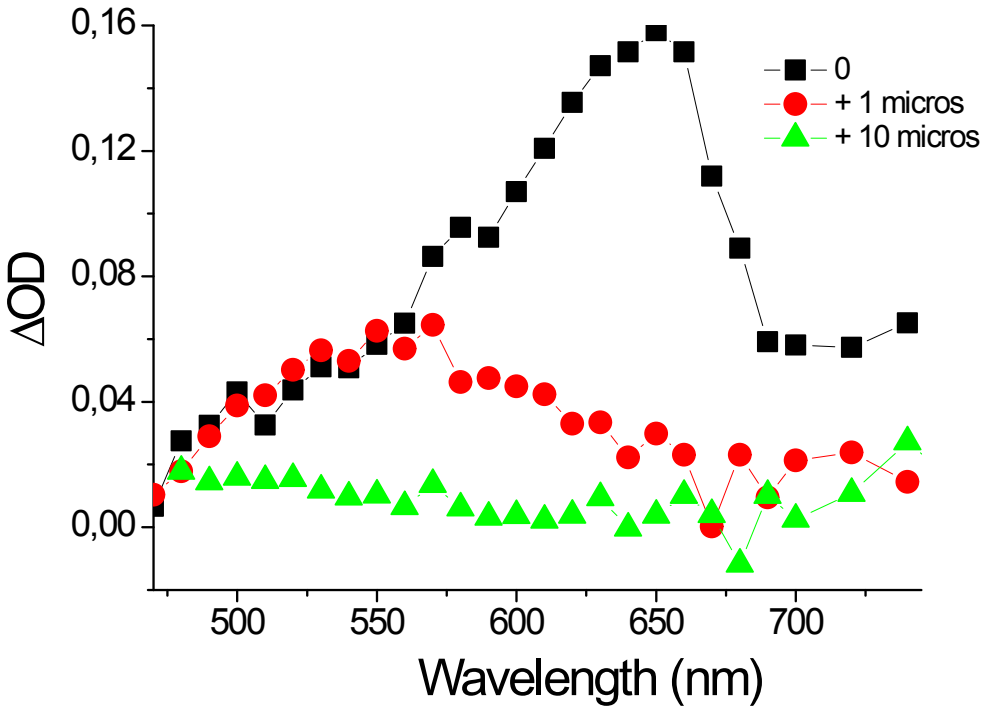

Figure S18. Transient absorption spectra of **TXA** in ACN solution after 0, 1 and 10 μs (λ_{ex} = 355 nm under argon atmosphere).

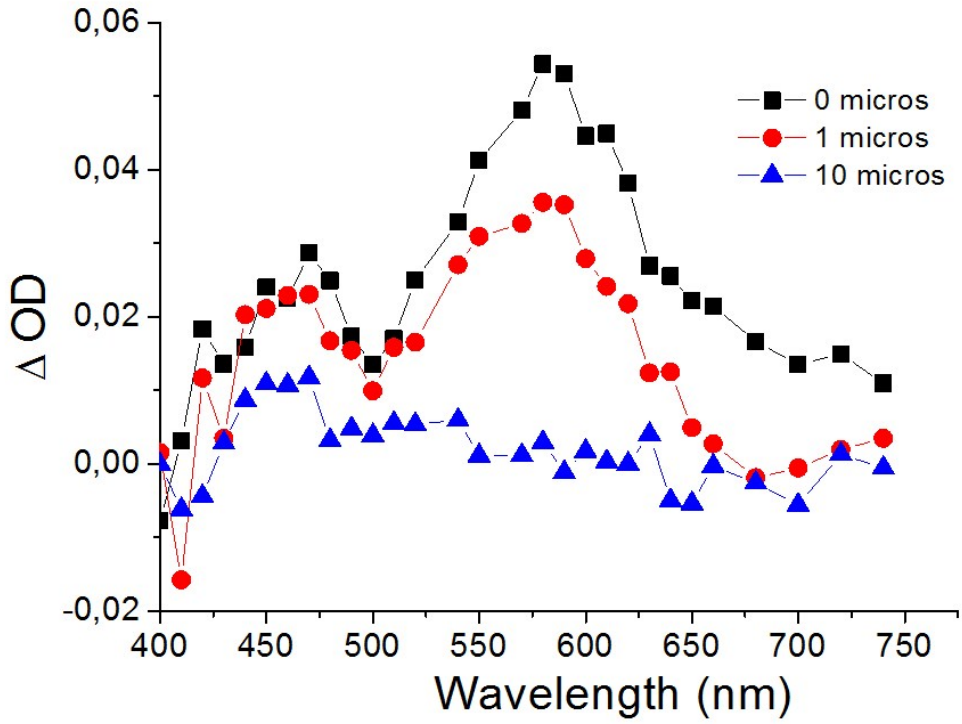

Figure S19. Transient absorption spectra of **TXo2A** in ACN solution after 0, 1 and 10 μs (λ_{ex} = 355 nm under argon atmosphere).

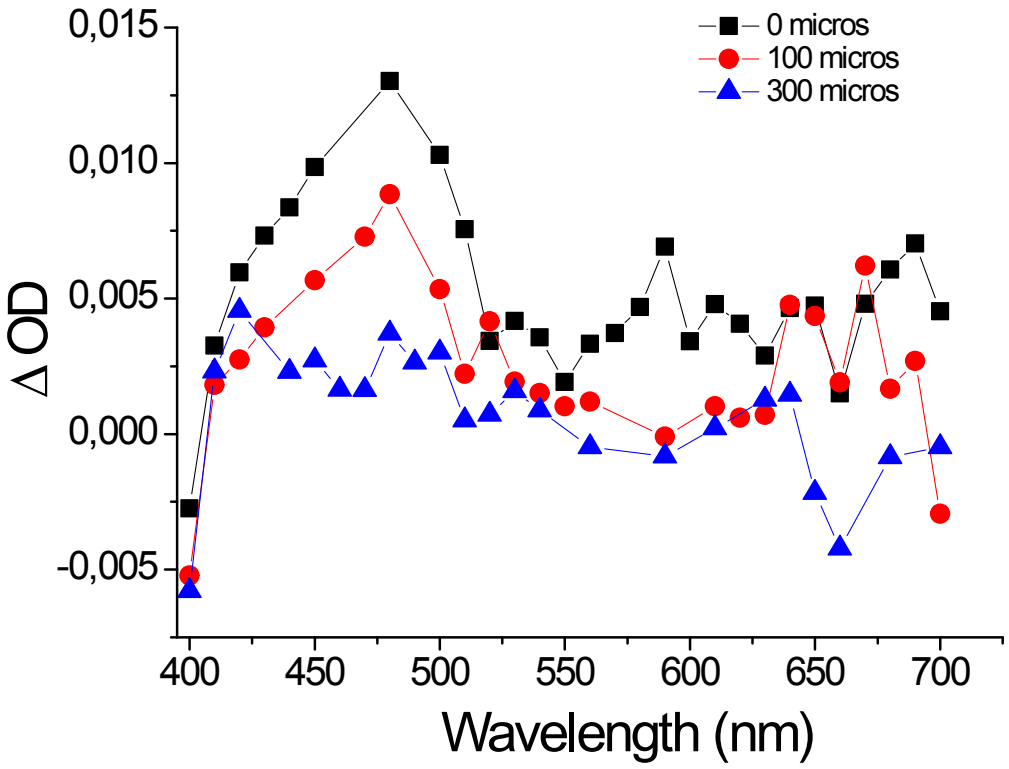

Figure S20. Transient absorption spectra of **TXBr** in THF solution after 0, 100 and 300 μs (λ_{ex} = 355 nm under argon atmosphere).

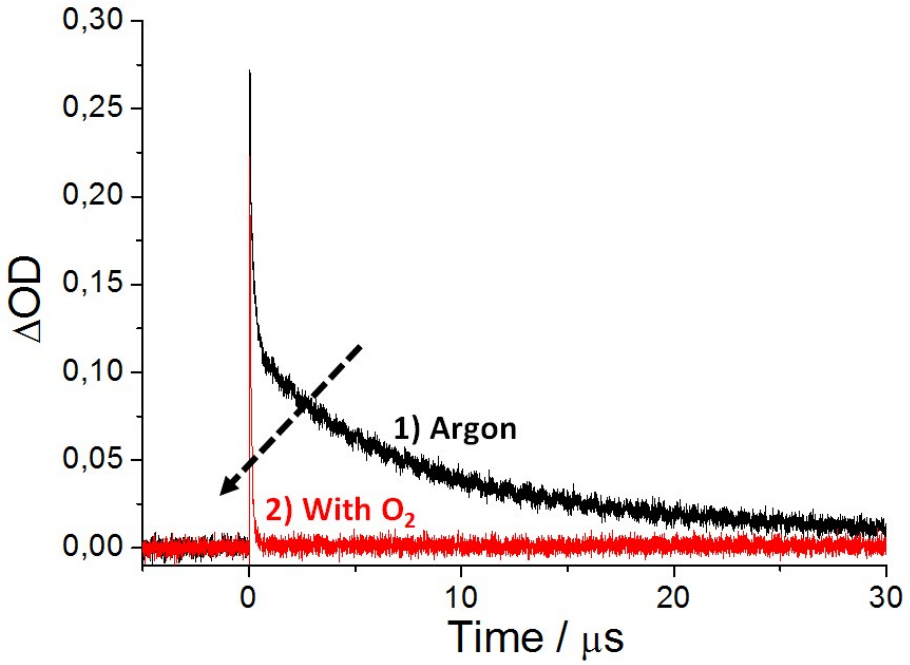

Figure S21. Decay traces of **TXA** triplet state (^{3}**TXA***) at 650 nm after a laser pulse (λ_{ex} = 355 nm) of argon (1) and O_2 (2) – saturated ACN solution of **TXA**.

.

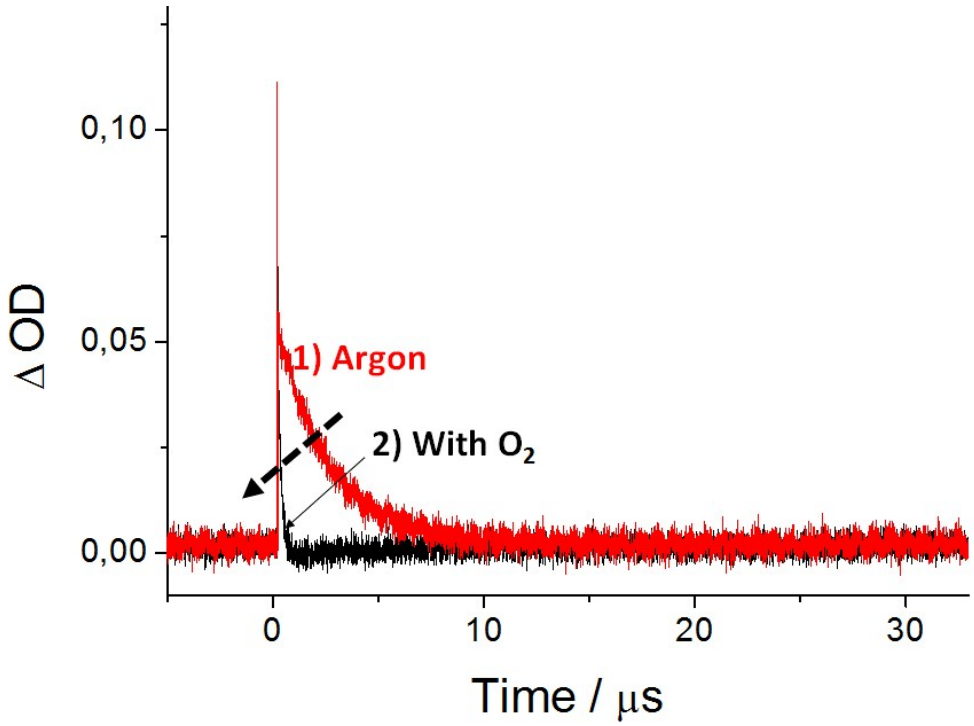

Figure S22. Decay traces of **TXo2A** triplet state (^{3}**TXo2A***) at 580 nm after a laser pulse (λ_{ex} = 355 nm) of argon (1) and O_2 (2) – saturated ACN solution of **TXo2A**.

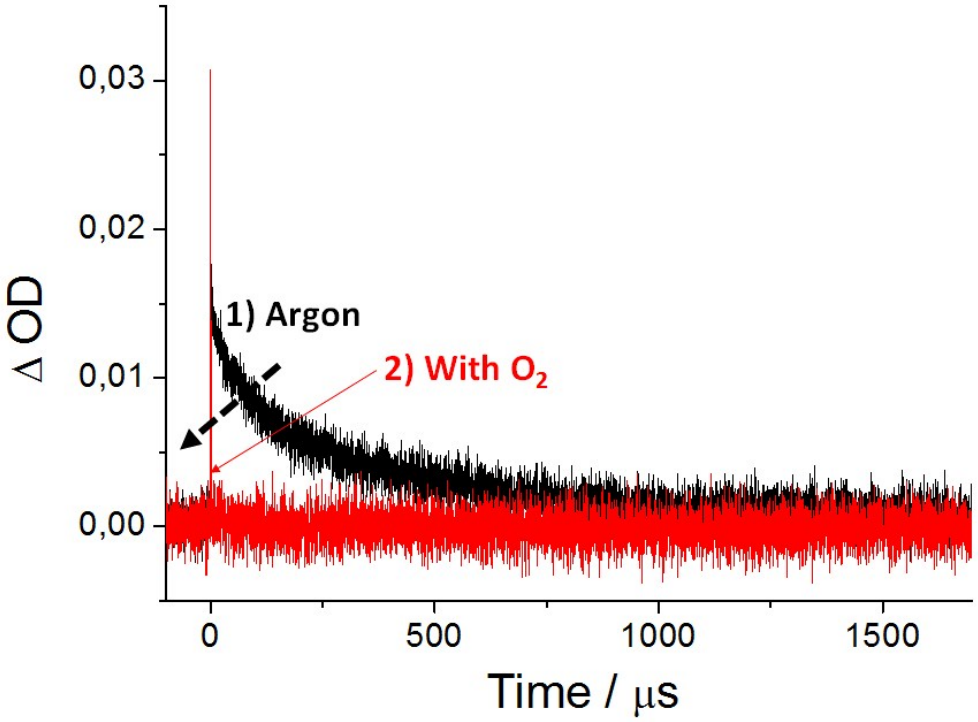

Figure S23. Decay traces of **TXBr** triplet state (^{3}**TXBr***) at 480 nm after a laser pulse (λ_{ex} = 355 nm) of argon (1) and O_2 (2) – saturated THF solution of **TXBr**.

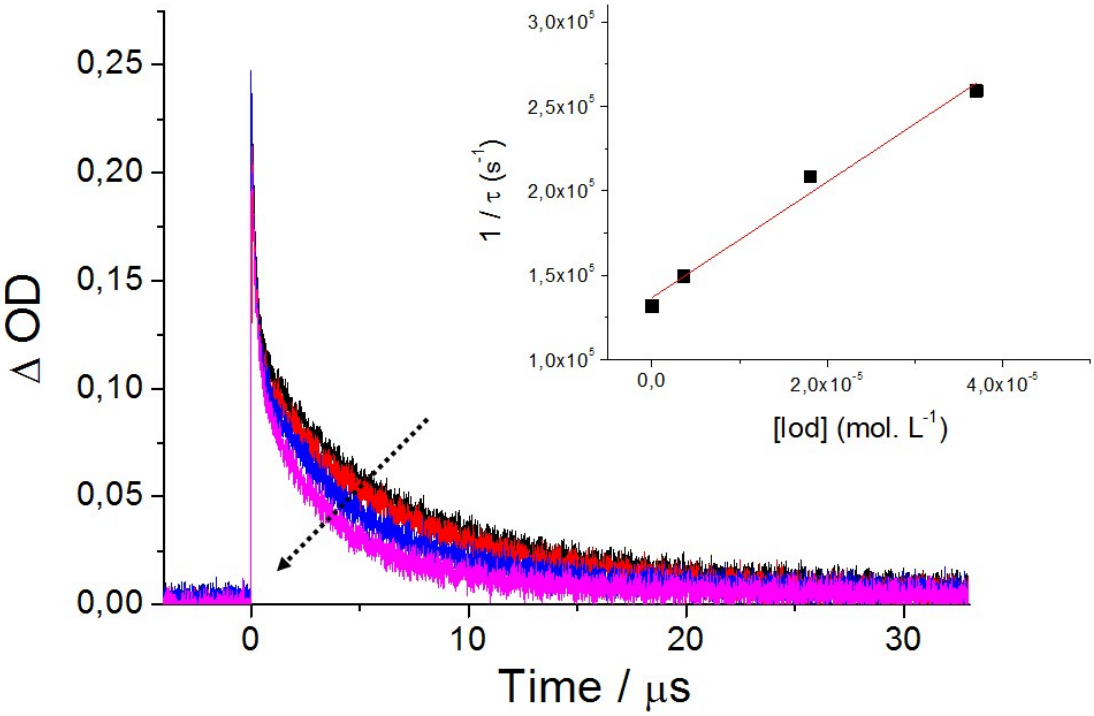

Figure S24. Decay traces of **TXA** triplet state (^{3}**TXA***) at 650 nm after the addition of Iod at different concentrations (0 M, 3.6 x 10^{-6} M, 1.8 x 10^{-5} M and 3.7 x 10^{-5} M) using LFP (λ_{ex} =

355 nm, 7 ns pulse width). Insert: Determination of the bimolecular quenching rate constants k_q of quenching of **TXA** triplet states by Iod. Pseudo-first-order decay rate constant of **TXA** triplet state absorbance monitored at 650 nm vs. varying concentration of Iod in ACN.

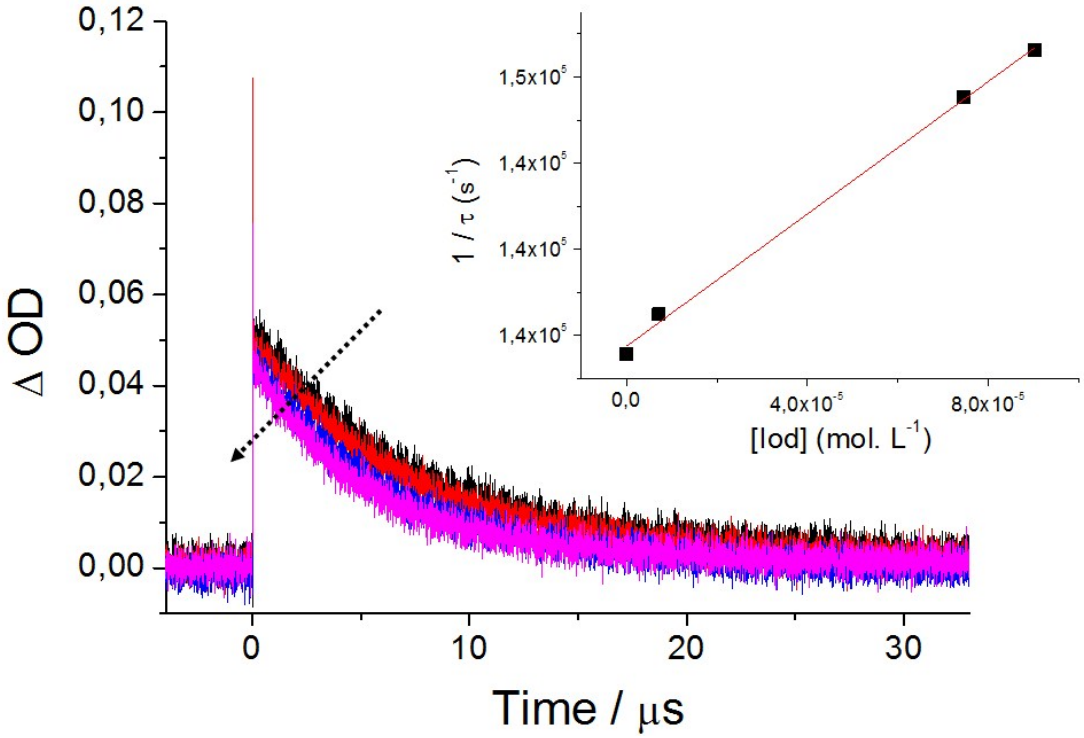

Figure S25. Decay traces of **TXo2A** triplet state (^{3}**TXo2A***) at 580 nm after the addition of Iod at different concentrations (0 M, 7.2 x 10^{-6} M, 7.45 x 10^{-5} M and 9 x 10^{-5} M) using LFP (λ_{ex} = 355 nm, 7 ns pulse width). Insert: Determination of the bimolecular quenching rate constants k_q of quenching of **TXo2A** triplet states by Iod. Pseudo-first-order decay rate constant of **TXo2A** triplet state absorbance monitored at 580 nm vs. varying concentration of Iod in ACN.

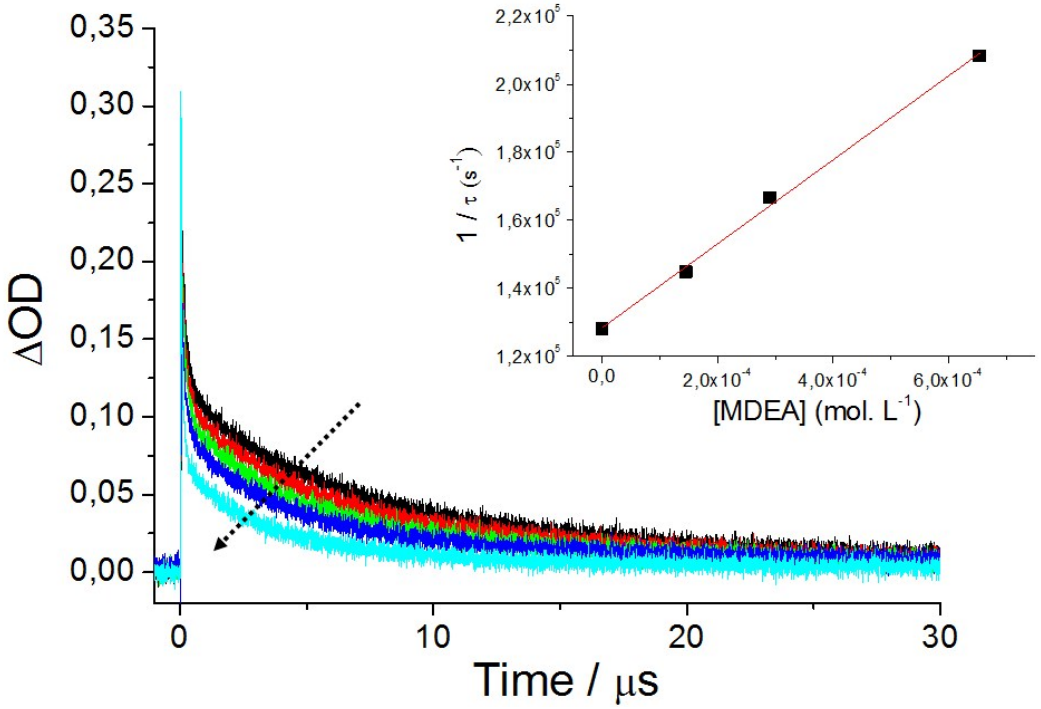

Figure S26. Decay traces of **TXA** triplet state (^{3}**TXA***) at 650 nm after the addition of MDEA at different concentrations (0 M, 1.45 x 10^{-4} M, 2.9 x 10^{-4} M and 6.54 x 10^{-4} M) using LFP (λ_{ex} = 355 nm, 7 ns pulse width). Insert: Determination of the bimolecular quenching rate constants k_q of quenching of **TXA** triplet states by MDEA. Pseudo-first-order decay rate constant of **TXA** triplet state absorbance monitored at 650 nm vs. varying concentration of MDEA in ACN.

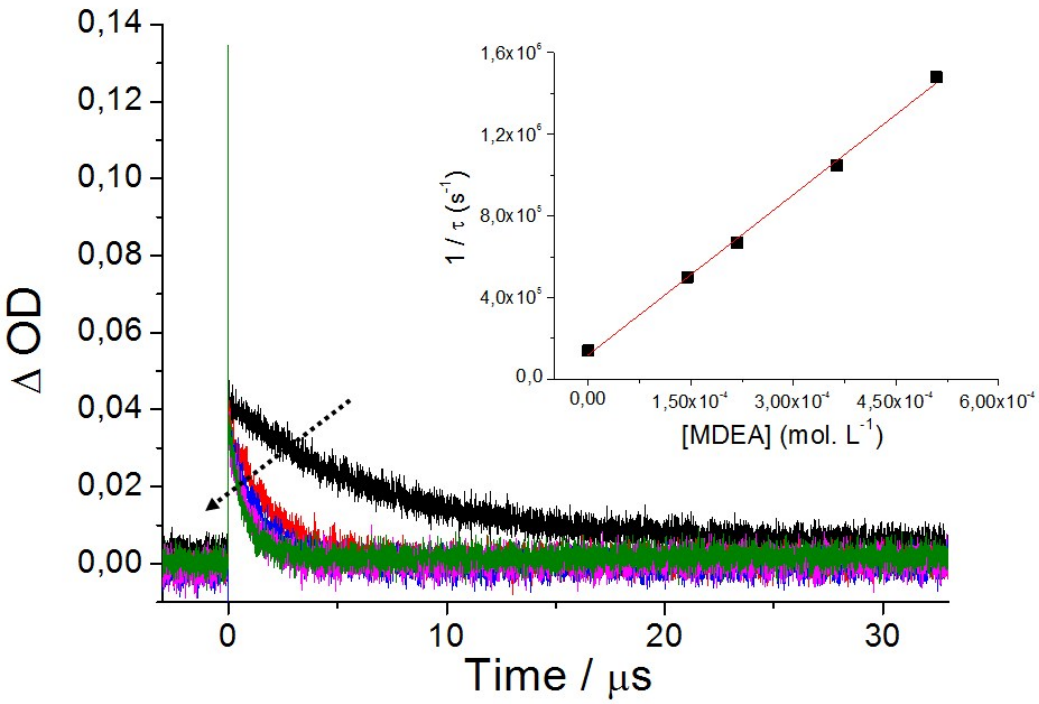

Figure S27. Decay traces of **TXo2A** triplet state (^{3}**TXo2A***) at 580 nm after the addition of MDEA at different concentrations (0 M, 1.45 x 10^{-4} M, 2.2 x 10^{-4} M, 3.6 x 10^{-4} and 5.1 x 10^{-4} M) using LFP (λ_{ex} = 355 nm, 7 ns pulse width). Insert: Determination of the bimolecular quenching rate constants k_q of quenching of **TXo2A** triplet states by MDEA. Pseudo-first-order decay rate constant of **TXo2A** triplet state absorbance monitored at 580 nm vs. varying concentration of MDEA in ACN.

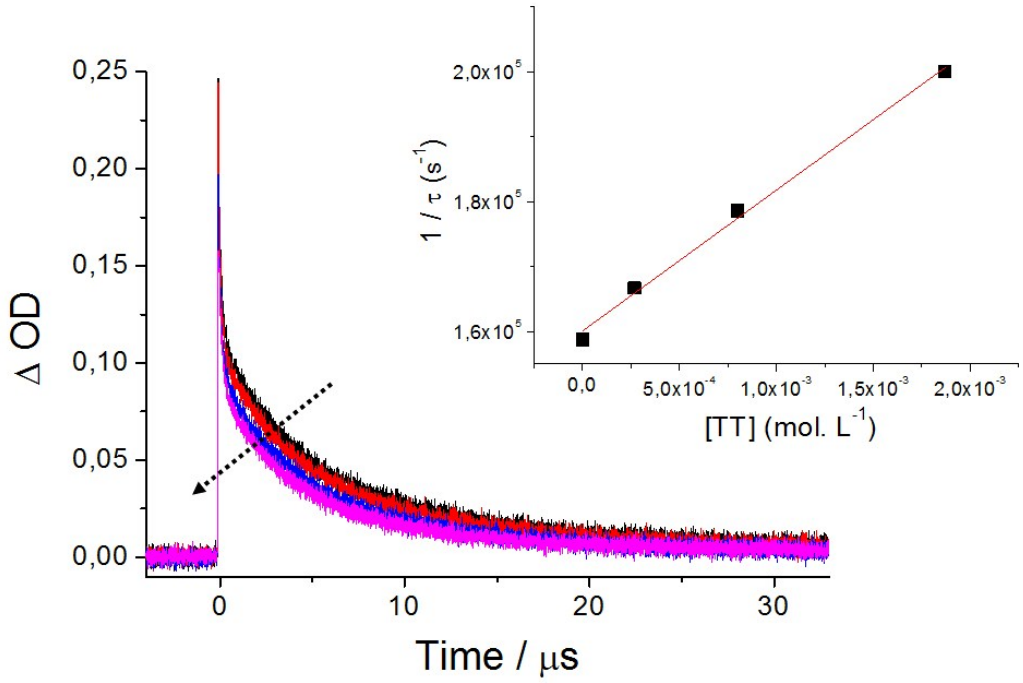

Figure S28. Decay traces of **TXA** triplet state (^{3}**TXA***) at 650 nm after the addition of TT at different concentrations (0 M, 2.7 x 10^{-4} M, 8 x 10^{-4} M and 1.9 x 10^{-3} M) using LFP (λ_{ex} = 355 nm, 7 ns pulse width). Insert: Determination of the bimolecular quenching rate constants k_q of quenching of **TXA** triplet states by TT. Pseudo-first-order decay rate constant of **TXA** triplet state absorbance monitored at 650 nm vs. varying concentration of TT in ACN.

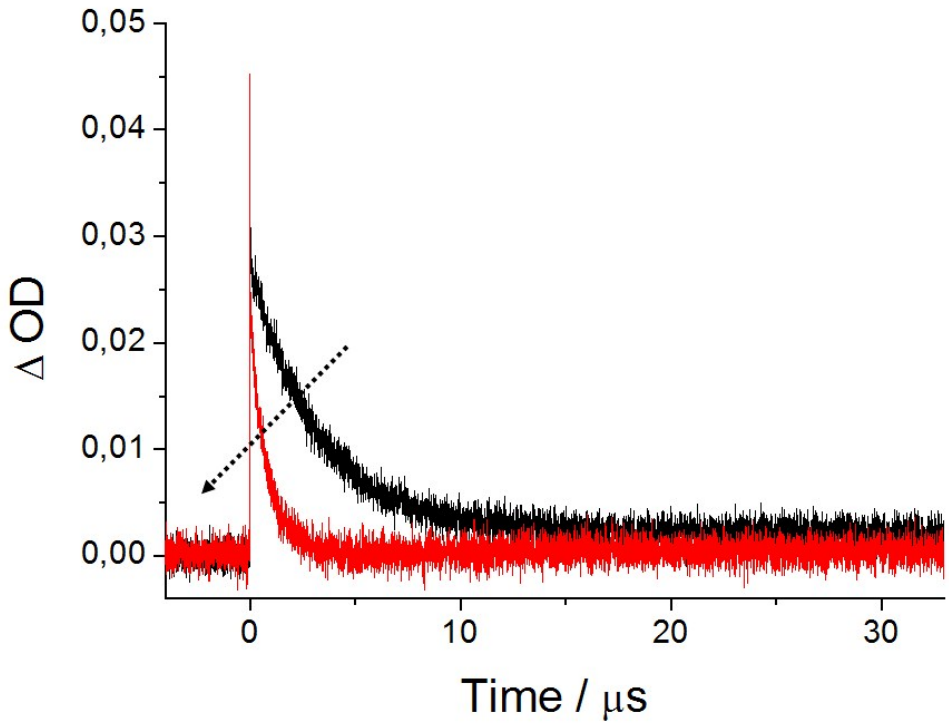

Figure S29. Decay traces of **TXo2A** triplet state (^{3}**TXo2A***) at 580 nm after the addition of TT at different concentrations (0 M and 12.5 mM) using LFP (λ_{ex} = 355 nm, 7 ns pulse width).

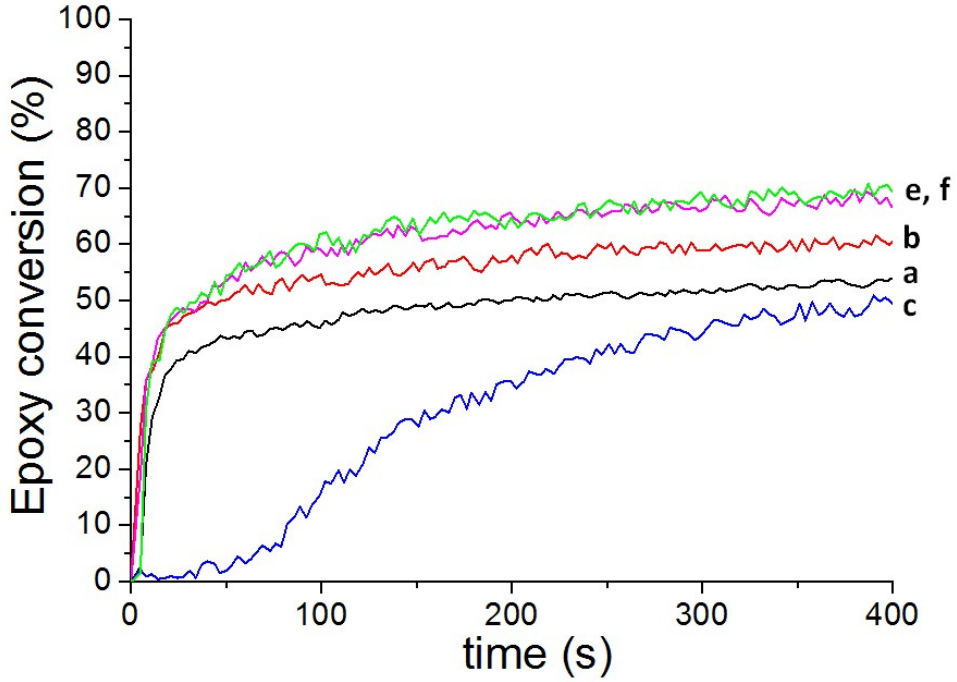

Figure S30. Kinetic profiles for the cationic polymerization of EPOX under air with **TXBr**/Iod (0.1%/1.5% w/w) upon LEDs irradiation at a) 385 nm, b) 405 nm, c) 455 nm; and compared

with TX/Iod (0.5%/1.5% w/w) system under air upon LEDs irradiation at e) 385 nm and f) 405 nm.

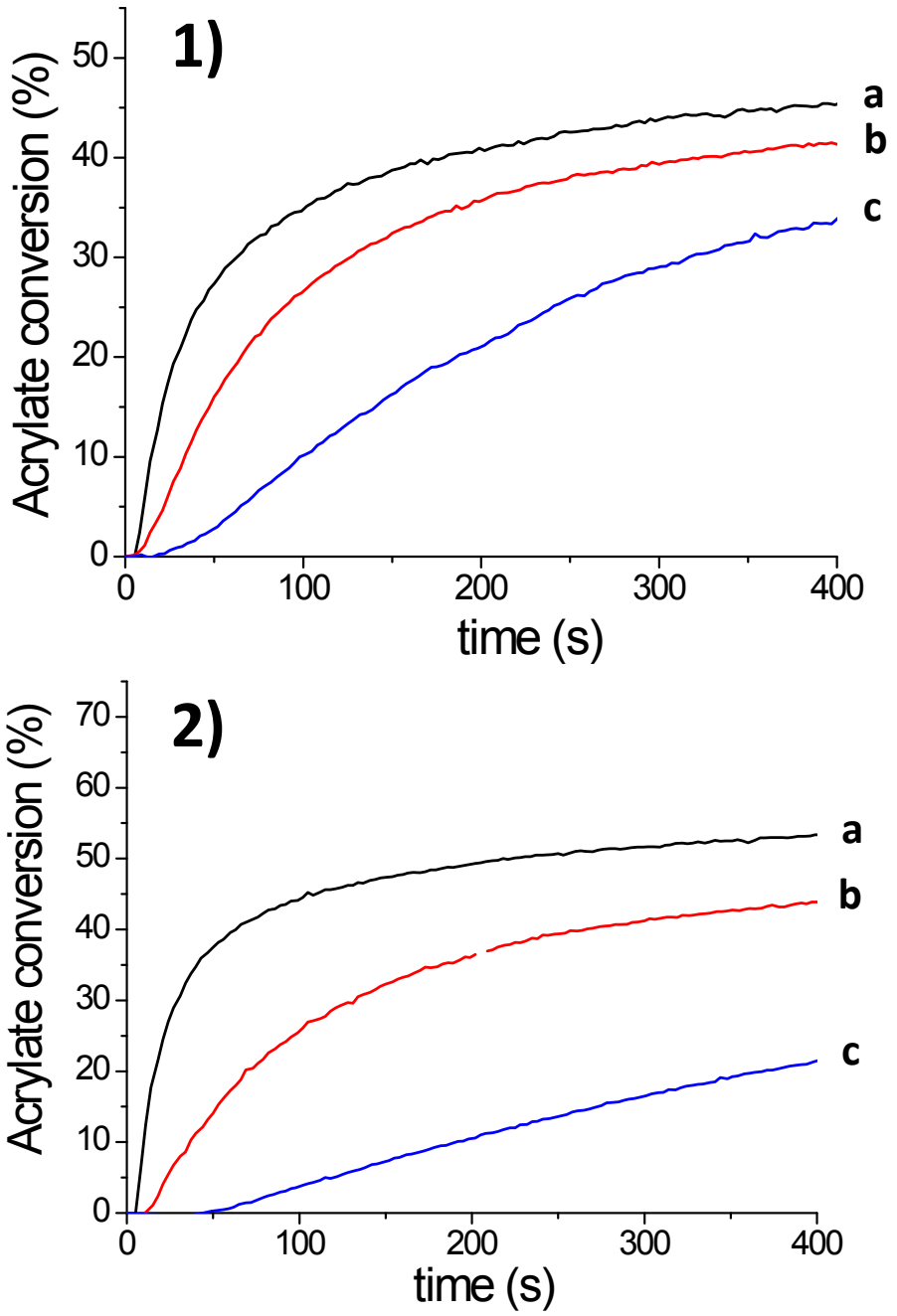

Figure S31. Kinetic profiles for the FRP of TMPTA in laminate with 1) **TXA** and 2) **TXo2A** upon LED exposure at a) 405 nm, b) 455 nm and c) 470 nm. [PI] = 0.5% wt.

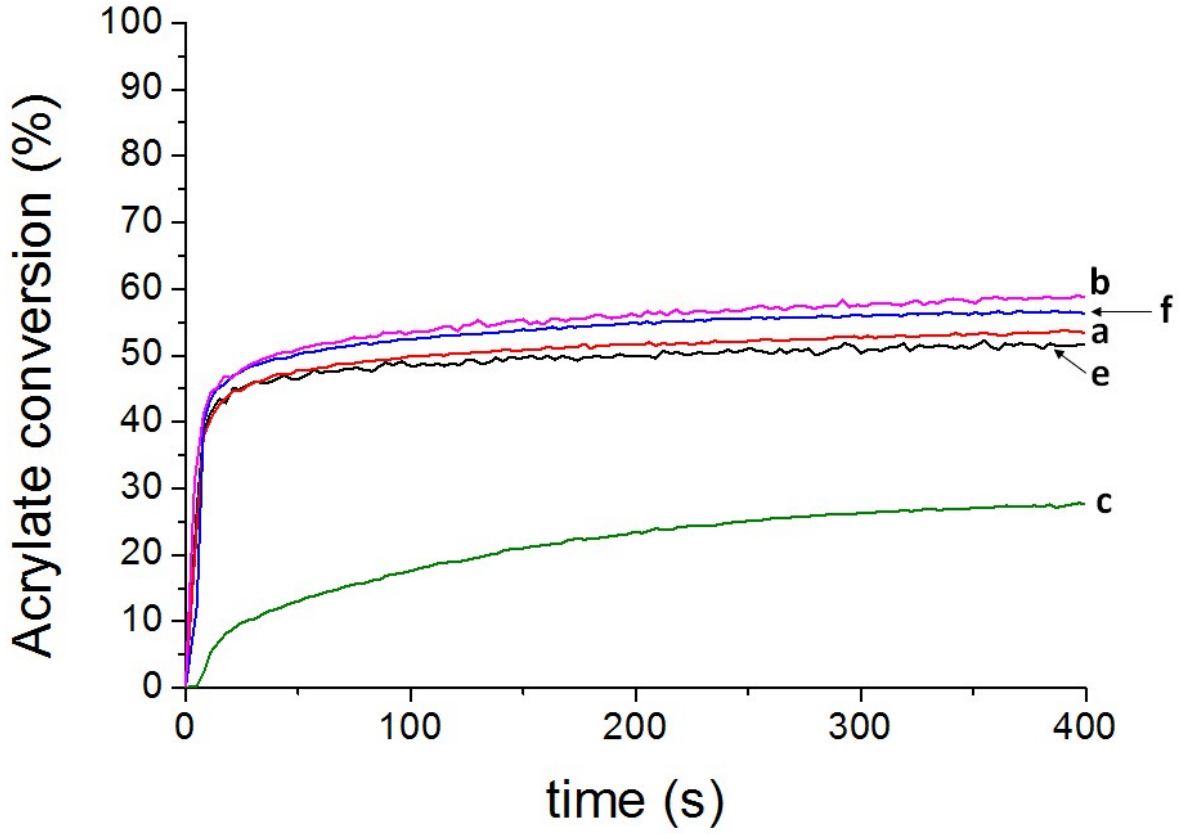

Figure S32. Kinetic profiles for the FRP of TMPTA with TX/MDEA (0.5%/3% w/w) upon LED exposure in laminate at a) 385 nm, b) 405 nm, c) 455 nm, and under air at e) 385 nm and f) 405 nm.

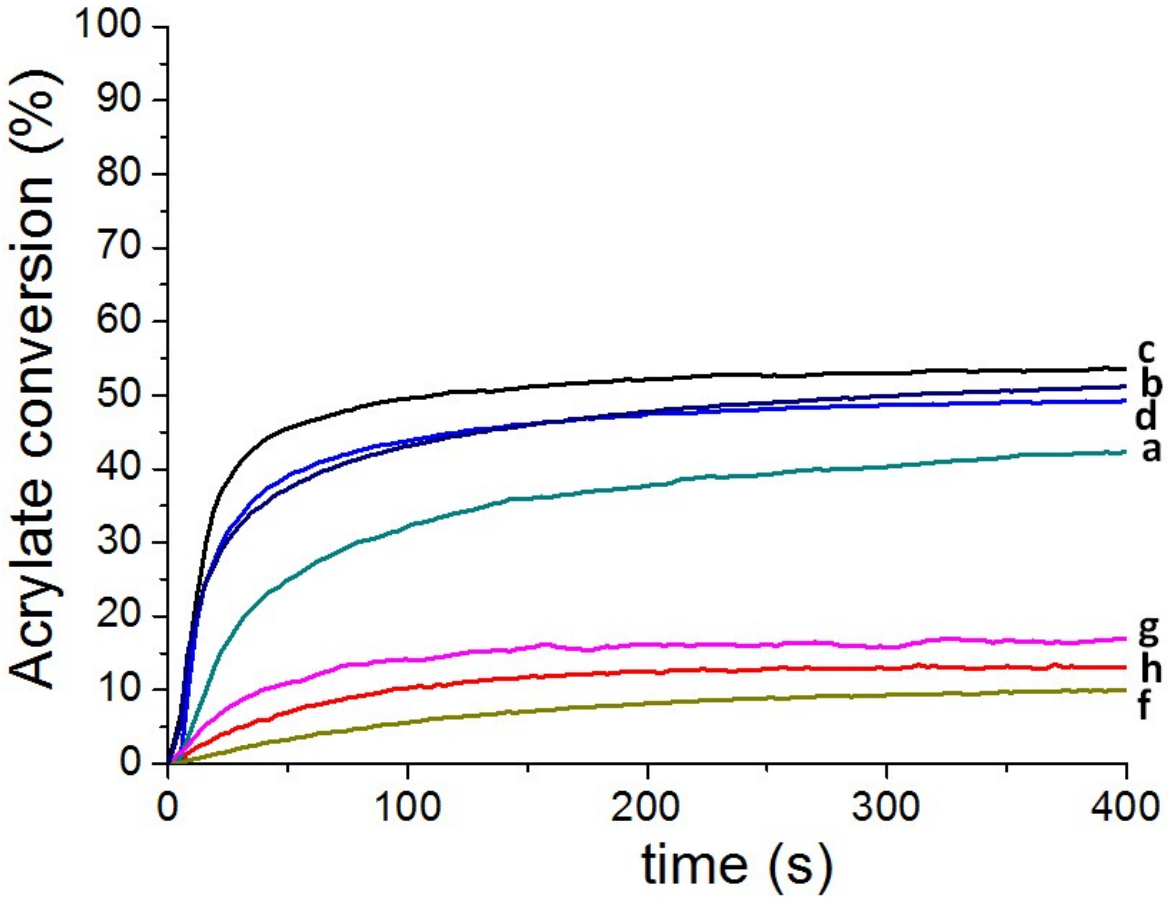

Figure S33. Kinetic profiles for the FRP of TMPTA with CQ/MDEA (0.5%/3% w/w) upon LED exposure in laminate at a) 385 nm, b) 405 nm, c) 455 nm and d) 470 nm, and under air at f) 405 nm, g) 455 nm and h) 470 nm.

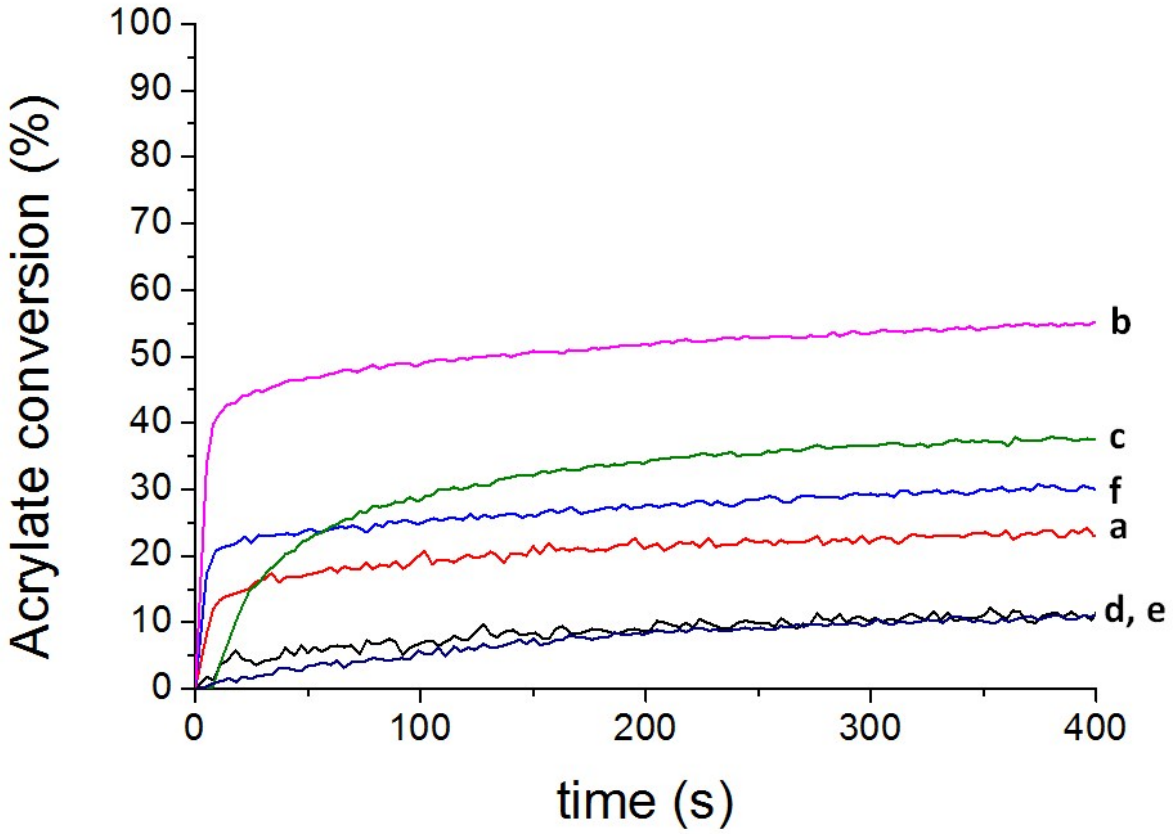

Figure S34. Kinetic profiles for the FRP of TMPTA with **TXBr**/MDEA (0.1%/3% w/w) upon LED exposure in laminate at a) 385 nm, b) 405 nm, c) 455 nm and d) 470 nm and under air at e) 385 nm and f) 405 nm.

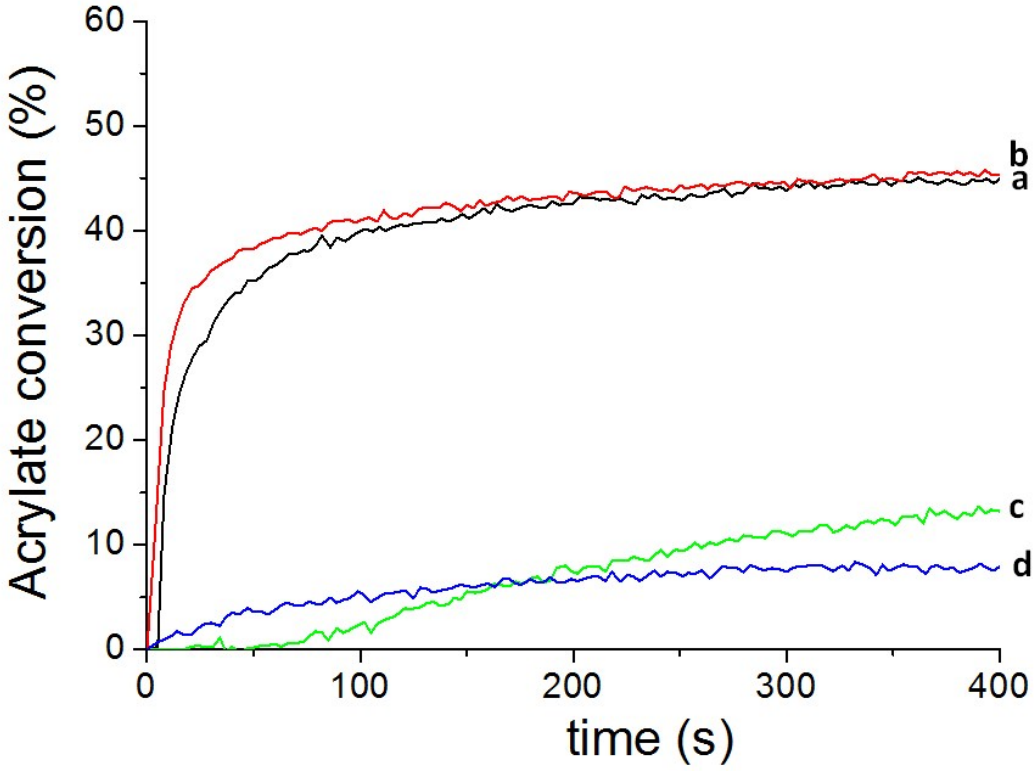

Figure S35. Kinetic profiles for the FRP of TMPTA with **TXBr**/Iod (0.1%/1.5% w/w) upon LED exposure in laminate at a) 385 nm, b) 405 nm, c) 455 nm and d) 470 nm. No polymerization under air.

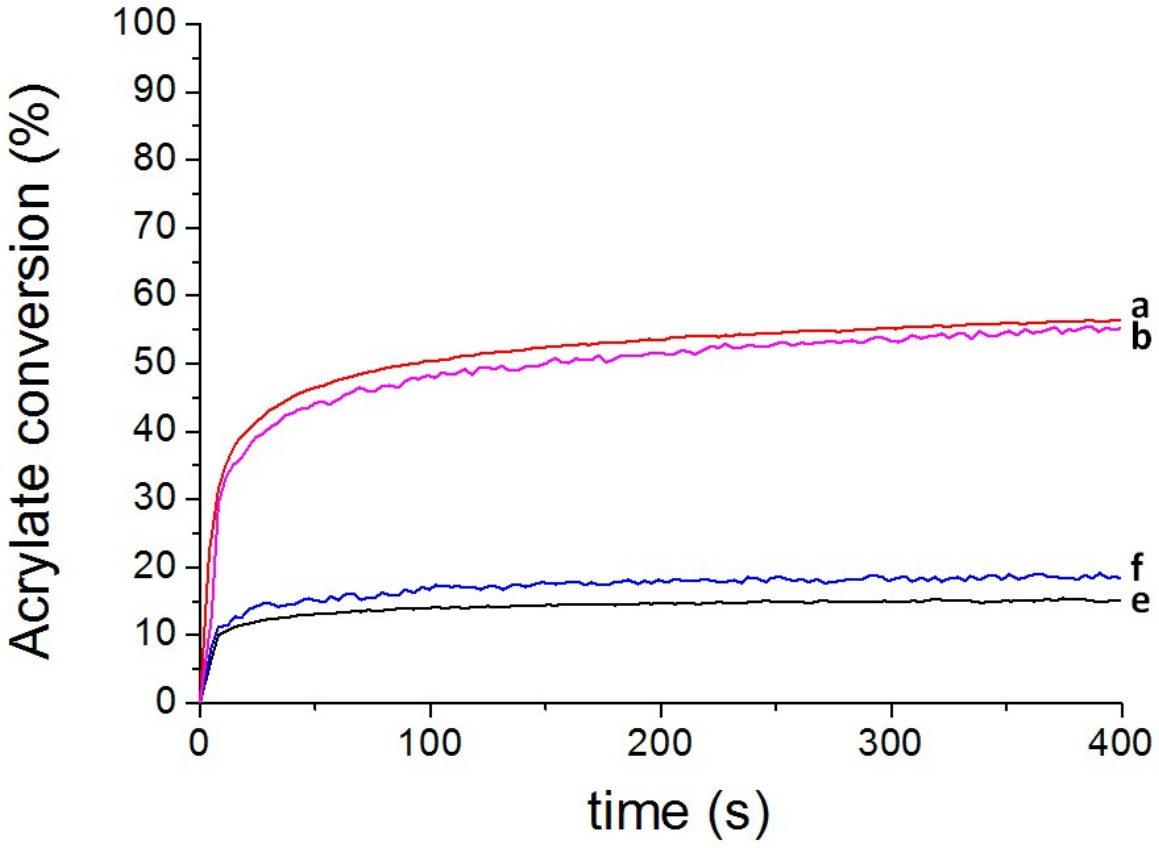

Figure S36. Kinetic profiles for the FRP of TMPTA with TX/Iod (0.5%/1.5% w/w) upon LED exposure in laminate at a) 385 nm and b) 405 nm, and under air at e) 385 nm and f) 405 nm.

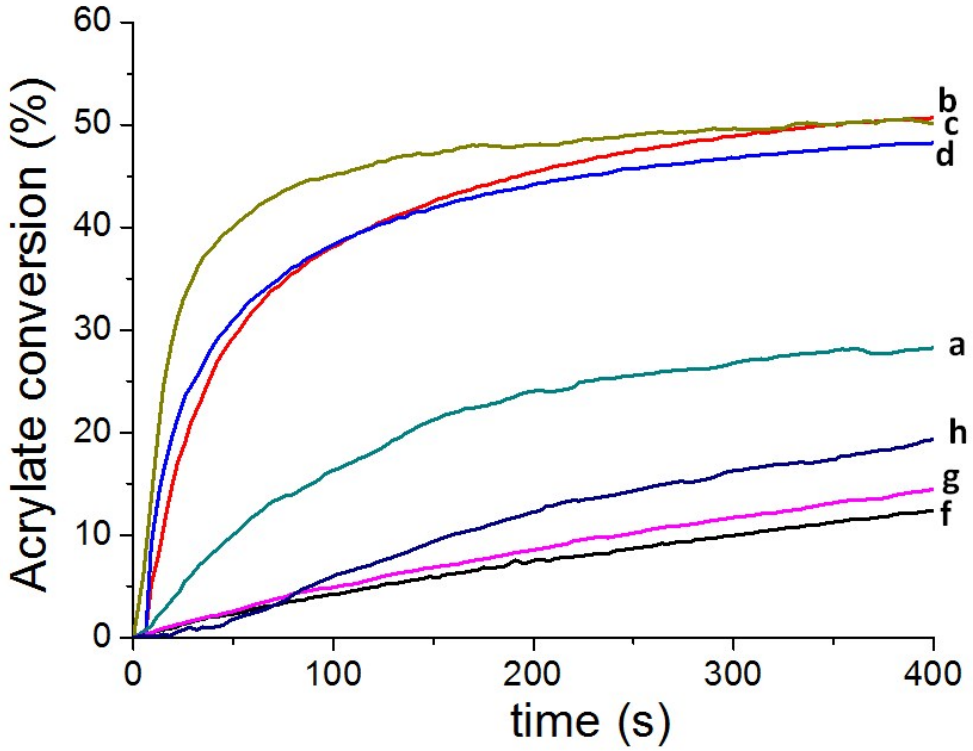

Figure S37. Kinetic profiles for the FRP of TMPTA with CQ/Iod (0.5%/1.5% w/w) upon LED exposure in laminate at a) 385 nm, b) 405 nm, c) 455 nm and d) 470 nm, and under air at e) 385 nm, f) 405 nm, g) 455 nm and h) 470 nm.

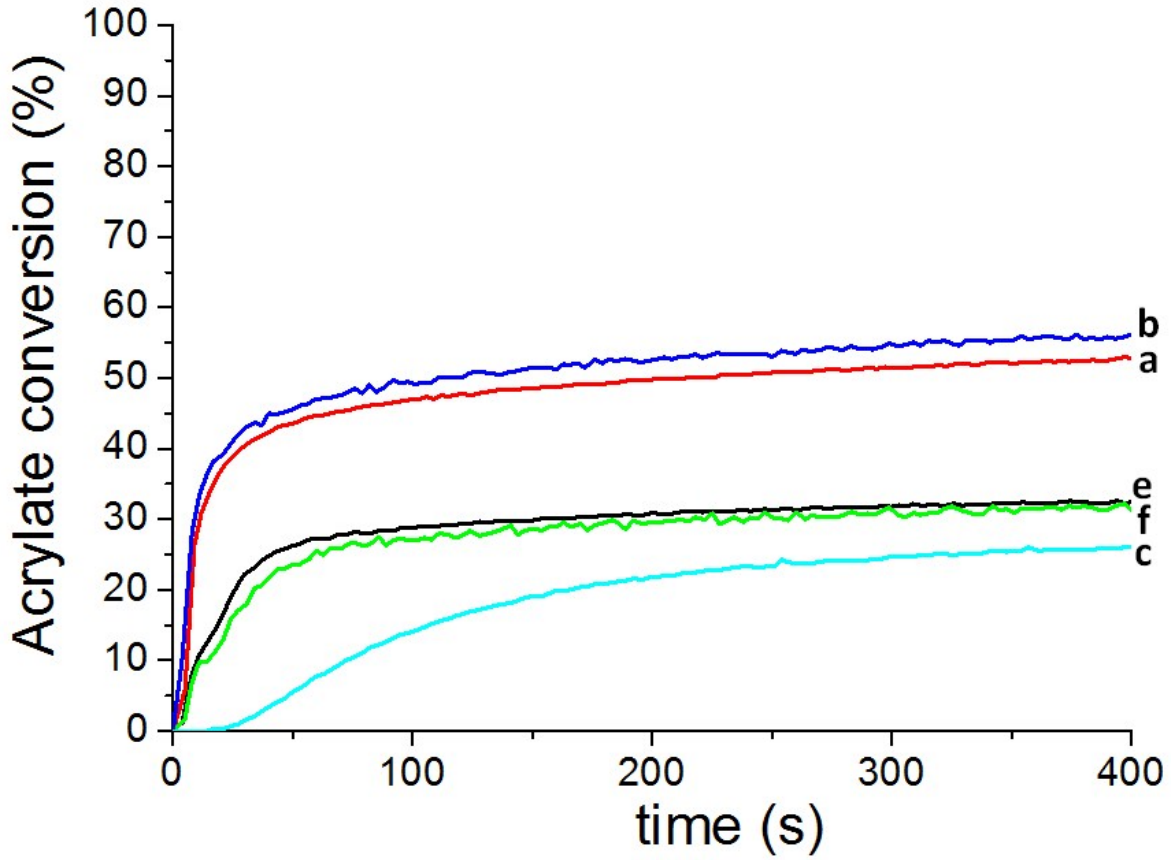

Figure S38. Kinetic profiles for the FRP of TMPTA with TX/TT (0.5%/3% w/w) upon LED exposure in laminate at a) 385 nm, b) 405 nm and c) 455 nm, and under air at e) 385 nm and f) 405 nm.

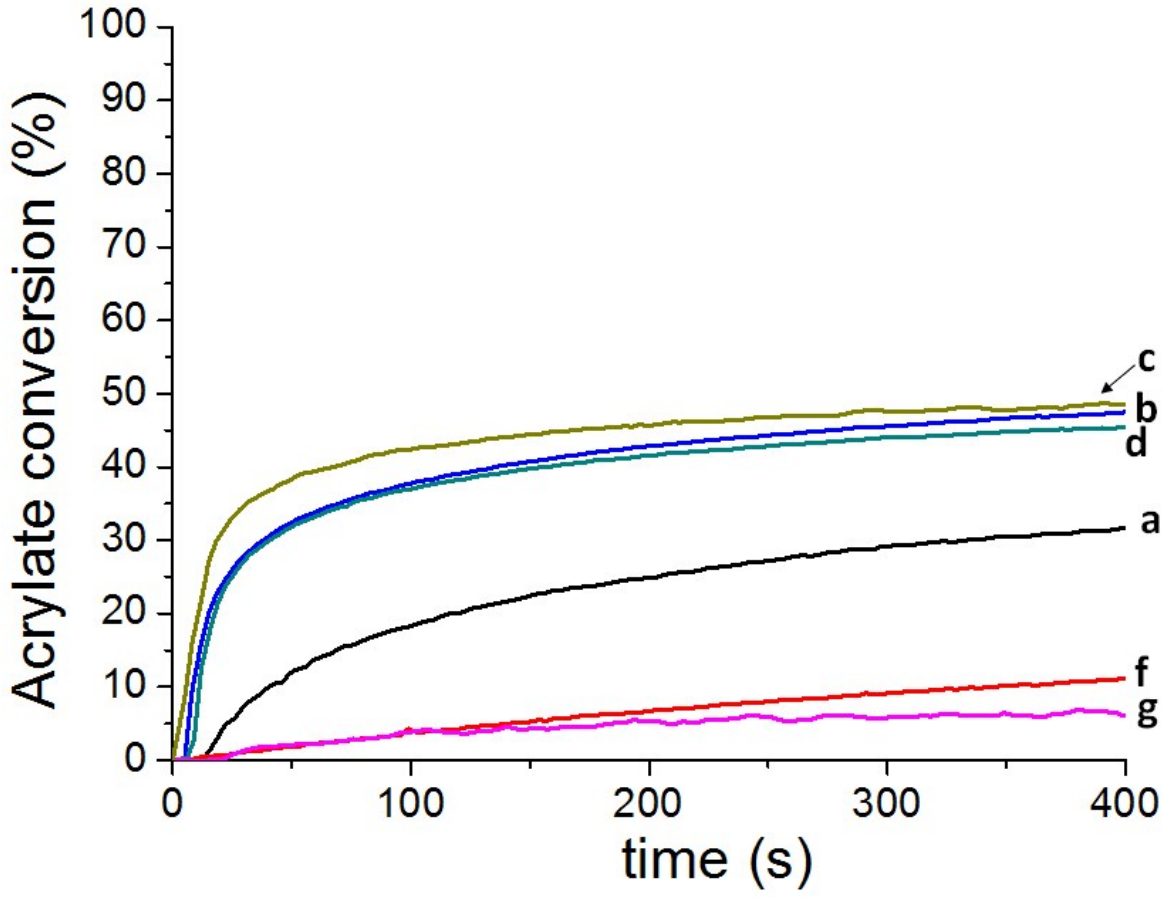

Figure S39. Kinetic profiles for the FRP of TMPTA with CQ/TT (0.5%/3% w/w) upon LED exposure in laminate at a) 385 nm, b) 405 nm, c) 455 nm and d) 470 nm, and under air at f) 405 nm and g) 455 nm.

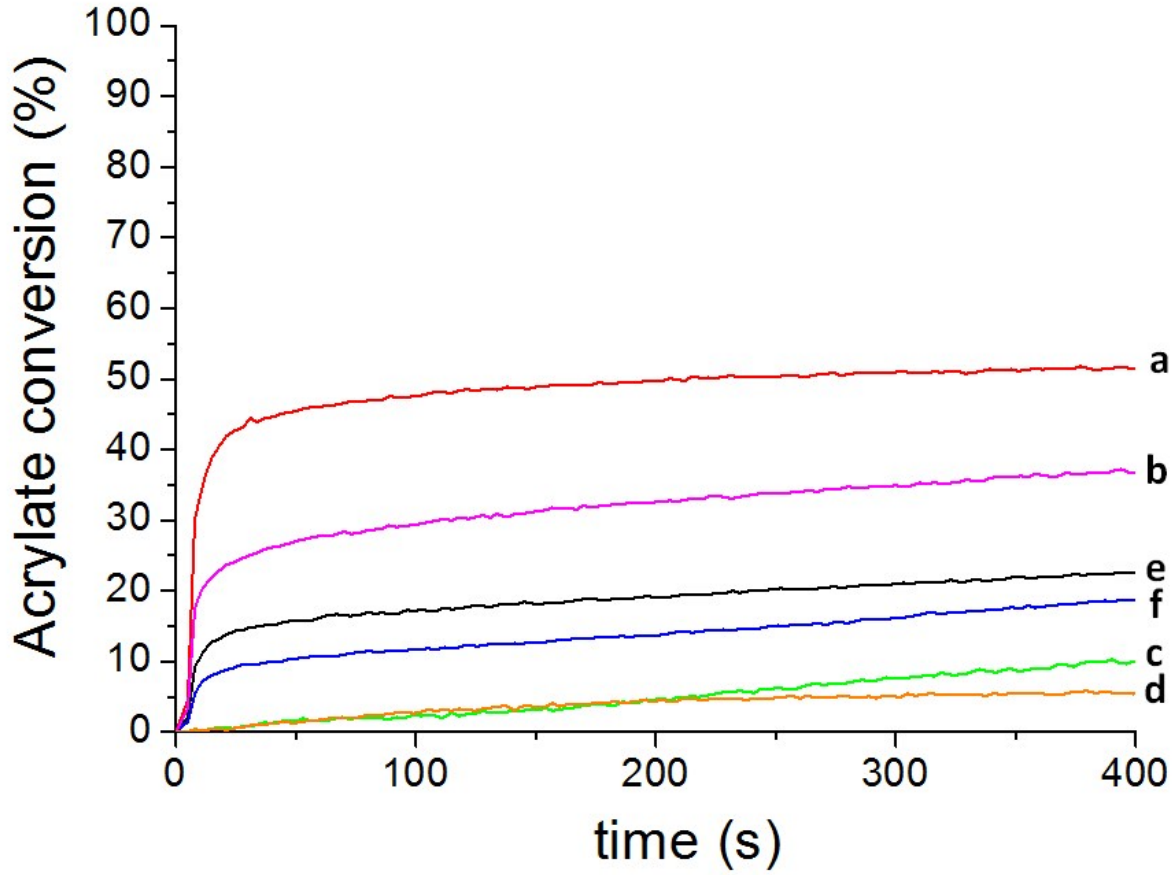

Figure S40. Kinetic profiles for the FRP of TMPTA with **TXBr**/TT (0.1%/3% w/w) upon LED exposure in laminate at a) 385 nm, b) 405 nm, c) 455 nm and d) 470 nm, and under air at e) 385 nm and f) 405 nm.

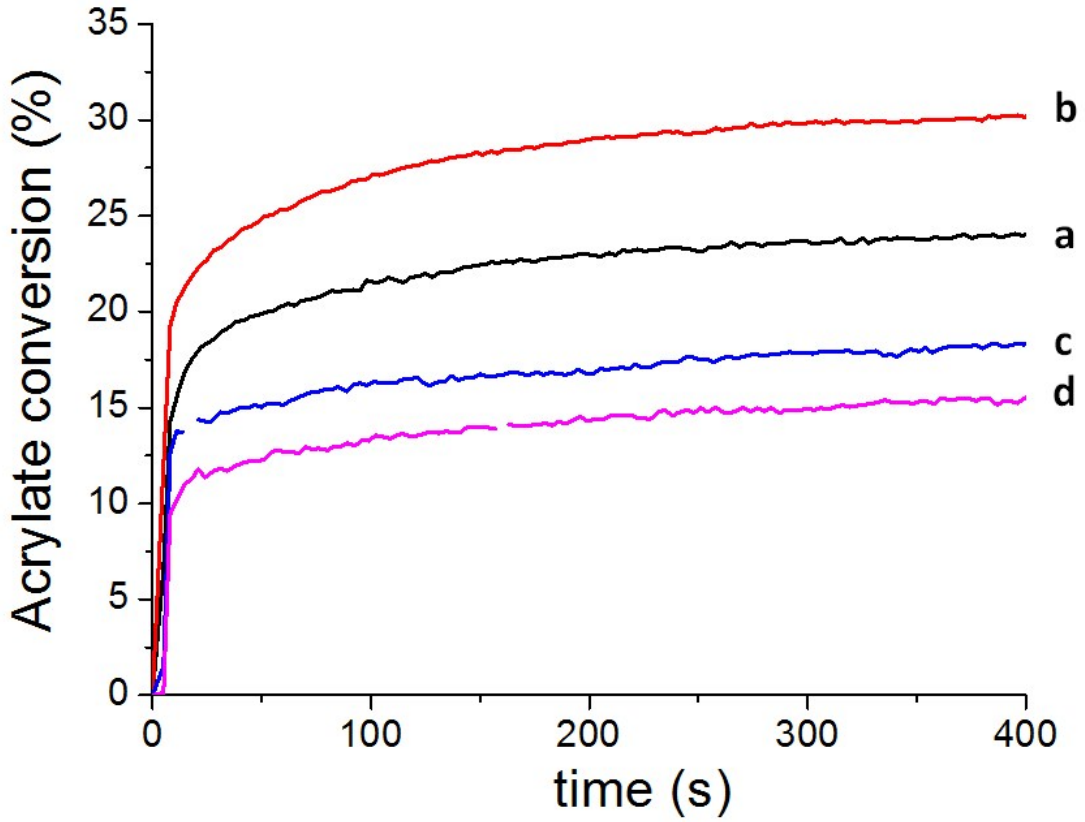

Figure S41. Kinetic profiles for the free-radical photopolymerization of TMPTA under air with **TXA**/Iod/TT (0.5%/1.5%/3% w/w) photoinitiating system upon LEDs@ a) 385 nm, b) 405 nm, c) 455 nm and d) 470 nm irradiation.

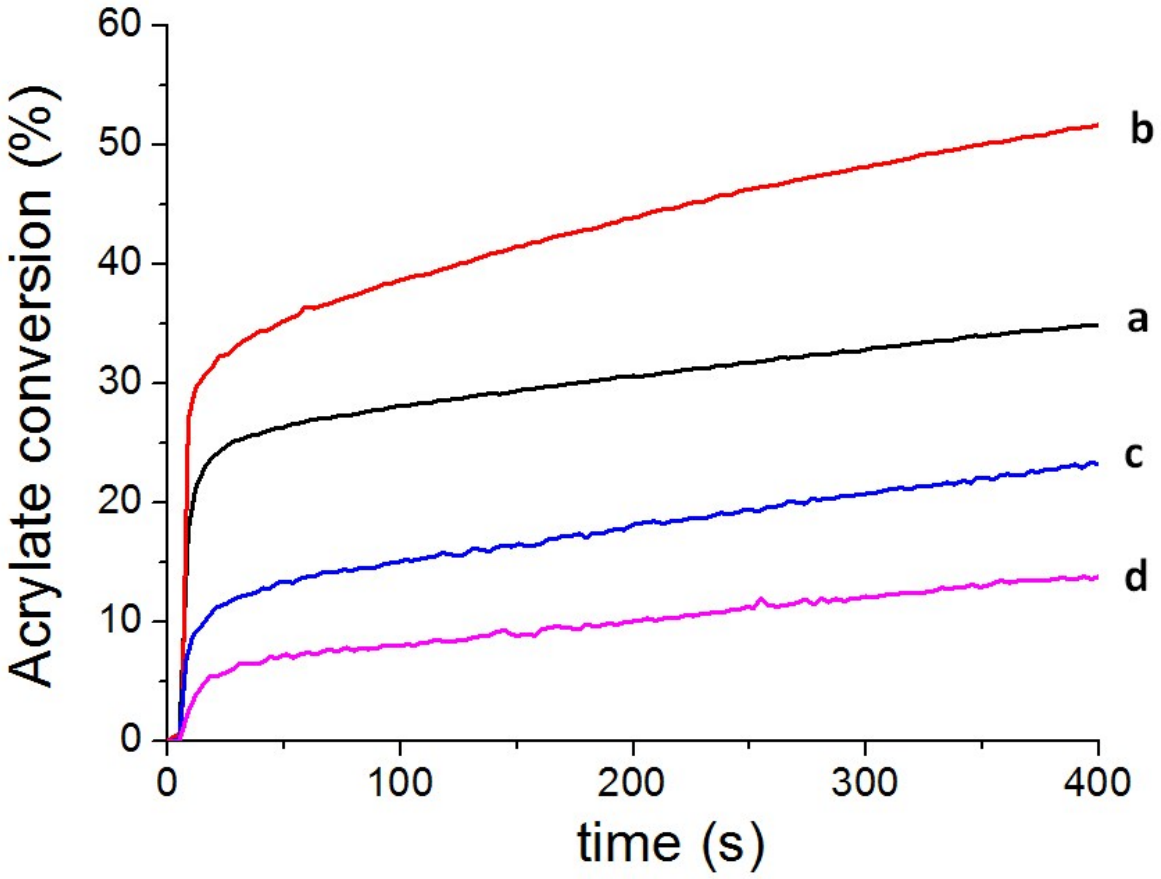

Figure S42. Kinetic profiles for the free-radical photopolymerization of TMPTA under air with **TXo2A**/Iod/TT (0.5%/1.5%/3% w/w) photoinitiating system upon LEDs@ a) 385 nm, b) 405 nm, c) 455 nm and d) 470 nm irradiation.

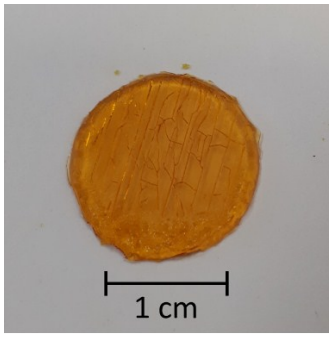

Figure S43. Optical image of a photopolymerized pellet from **TXo2A**/Iod/EPOX/TMPTA formulation.

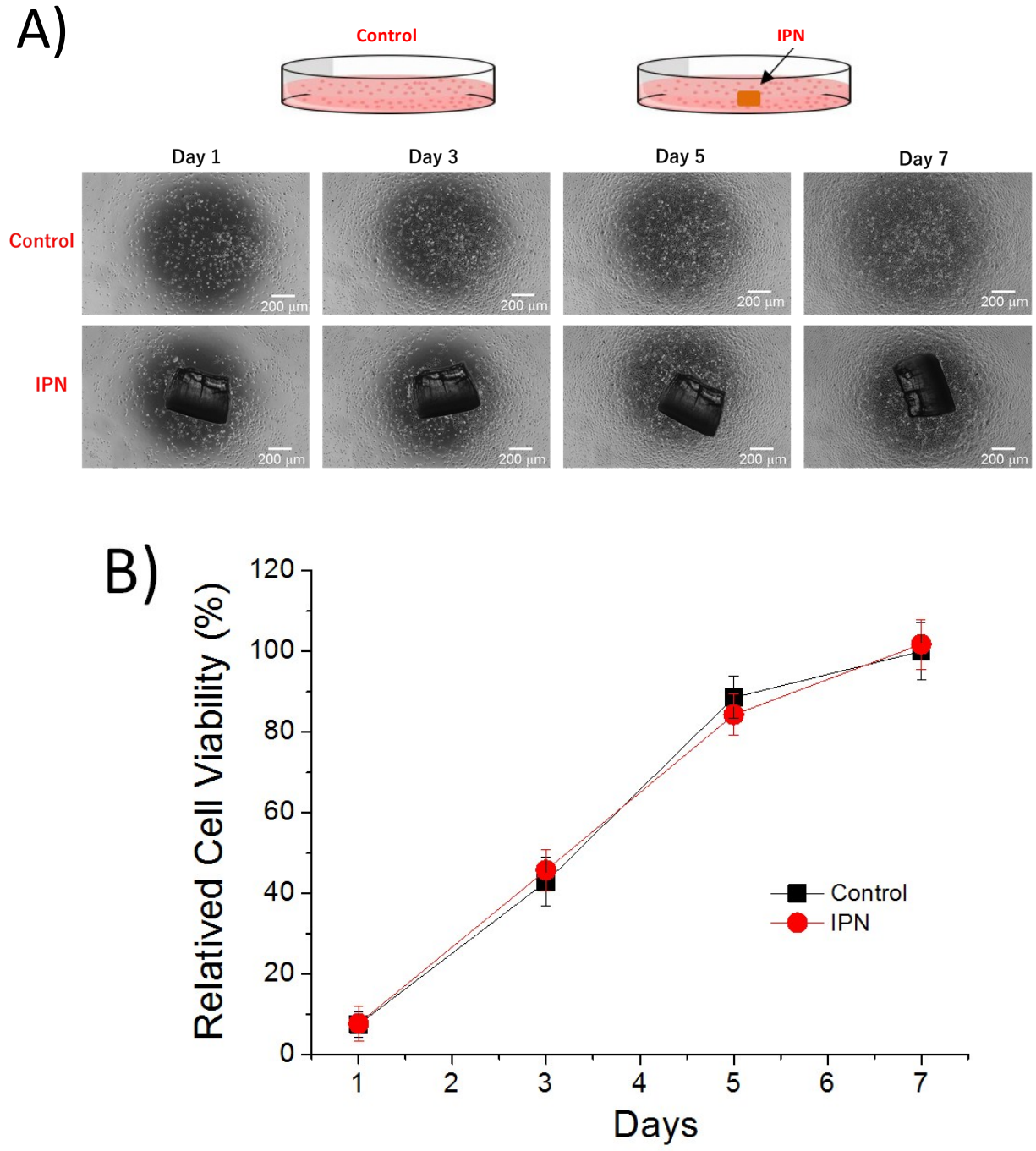

Figure S44. A) Phase contrast images of NIH/3T3 cells without IPN sample (control) and with IPN sample (**TXo2A**/Iod/TMPTA/EPOX) after 1, 3, 5, and 7 days of culture. B) Proliferation assay of NIH/3T3 cells without (square) or with (round) IPN sample on the cell culture dish.

TABLES

Table S1. Spectroscopic data (absorption, fluorescence and phosphorescence) of thioxanthone and its derivatives, calculated at B3LYP/6-311++G**//B3LYP/6-31+G* level of theory. Both vertical transition energies (λ) and intensities (*f*, oscillator strengths) are shown. *f* is not calculated for phosphorescence, corresponding to a formally spin-forbidden transition. Solvents: acetonitrile (ACN); tetrahydrofuran (THF).

Compound	Solvent	λ_{abs} (nm)	$f \cdot 10^{-3}$	λ_{fluo} (nm)	$f \cdot 10^{-3}$	λ_{phosph} (nm)
TX	ACN	359	116			
TXBr	ACN	376	97.2	421	71.0	497
TXBr	THF	376	99.6	419	73.5	491
TXA	ACN	446	88.2	544	69.6	647
TXo2A	ACN	426, 469	56.5, 7.80	584	9.80	623